AD_____
(Leave blank)

Award Number:

W81XWH-04-1-0106

TITLE:

Glutamate Receptor Aptamers and ALS

PRINCIPAL INVESTIGATOR:

Li Niu, Ph.D.

CONTRACTING ORGANIZATION:

The Research Foundation of SUNY
Albany, New York 12222

REPORT DATE:

January 2009

TYPE OF REPORT:

Annual

PREPARED FOR: U.S. Army Medical Research and Materiel Command
Fort Detrick, Maryland 21702-5012

DISTRIBUTION STATEMENT: (Check one)

X Approved for public release; distribution unlimited

Distribution limited to U.S. Government agencies only; report contains proprietary information

REPORT DOCUMENTATION PAGE

Form Approved
OMB No. 0704-0188

1. REPORT DATE *(DD-MM-YYYY)*	2. REPORT TYPE	3. DATES COVERED *(From - To)*
07-01-2009	Annual	*8 DEC 2007 - 7 DEC 2008

4. TITLE AND SUBTITLE

Glutamate Receptor Aptamers and ALS

5a. CONTRACT NUMBER
W81XWH-04-1-0106

5b. GRANT NUMBER

5c. PROGRAM ELEMENT NUMBER

6. AUTHOR(S)

Li Niu

5d. PROJECT NUMBER

5e. TASK NUMBER

5f. WORK UNIT NUMBER

7. PERFORMING ORGANIZATION NAME(S) AND ADDRESS(ES)

The Research Foundation of SUNY

Albany, New York 12222

8. PERFORMING ORGANIZATION REPORT NUMBER

9. SPONSORING / MONITORING AGENCY NAME(S) AND ADDRESS(ES)

U.S. Army Medical Research and Materiel Command
Fort Detrick, Maryland 21702-5012

10. SPONSOR/MONITOR'S ACRONYM(S)

11. SPONSOR/MONITOR'S REPORT NUMBER(S)

12. DISTRIBUTION / AVAILABILITY STATEMENT

Approved for public release; distribution unlimited

13. SUPPLEMENTARY NOTES

14. ABSTRACT

Excitotoxicity is one of the leading causes for amyotrophic lateral sclerosis (ALS). Our goal was to develop a novel class of powerful aptamer-based, anti-excitotoxic inhibitors against GluR2Qflip, a key AMPA receptor subunit that controls the calcium permeability and mediates excitotoxicity. An aptamer is a single-stranded nucleic acid that directly inhibits a protein's function by folding into a specific tertiary structure that dictates high-affinity binding to the target protein. To date, we have identified two classes of aptamers (i.e. competitive and noncompetitive aptamers) against GluR2Qflip, by using a molecular biology approach called systematic evolution of ligands by exponential enrichment (SELEX). These aptamers are water soluble and have a nanomolar affinity against GluR2Qflip. Their inhibitory properties rival those of any existing small, chemical inhibitors. We are continuing to work with these aptamers towards developing them into anti-excitotoxic drugs for treating patients with ALS, including those Gulf War veterans suffering from ALS.

15. SUBJECT TERMS
ALS, anti-excitotoxic drugs, SELEX, aptamers, glutamate receptors

16. SECURITY CLASSIFICATION OF:			17. LIMITATION OF ABSTRACT	18. NUMBER OF PAGES	19a. NAME OF RESPONSIBLE PERSON
a. REPORT	b. ABSTRACT	c. THIS PAGE			USAMRMC
U	U	U	UU	30	19b. TELEPHONE NUMBER *(include area code)*

Table of Contents

	Page
Introduction	**4-5**
Body	**5-15**
Key Research Accomplishments	**16**
Reportable Outcomes	**16-18**
Conclusion	**18-19**
References	**19-20**
Appendices	**21-30**

1. INTRODUCTION

This funded research is to discover novel aptamer candidates as potential drugs for a new therapy for amyotrophic lateral sclerosis (ALS). Previous studies of the first Gulf War veterans with ALS suggest a direct link of the Gulf War combat service to this fatal neurodegenerative disease. Although a number of pathogenic theories have been proposed, including oxidative stress, excitotoxicity, mitochondrial dysfunction, etc., the cause(s) of the disease, including the pathogenesis of the war-related ALS, is unknown, other than in ~10% cases of familial disease arising from mutations in the superoxide dismutase 1 gene (SOD1). However, excitotoxicity or excessive excitatory neurotransmission, mainly mediated by the AMPA-type (α-amino-3-hydroxy-5-methyl-4-isoxazole propionate) glutamate receptors, is thought to play a central role in the selective motor neuron death in ALS. In fact, riluzole, the only therapeutic drug available for ALS patients, albeit with a marginal effect on survival, is actually an inhibitor of presynaptic glutamate release. Therefore, developing AMPA receptor inhibitors to control the receptor-mediated neurodegeneration is a logical therapeutic approach. Traditionally, the main strategy in inhibitor/drug design has been by organic synthesis to make small molecule inhibitors. However, the majority of these synthetic inhibitors are poorly water soluble, and some prominent compounds, such as NBQX, a classical competitive inhibitor of AMPA/kainate receptors and one of the most potent inhibitors ever developed, have failed clinically because of the poor water solubility.

The hypothesis to be tested in this proposal is that potent and selective AMPA receptor inhibitors (aptamers) can be developed by a novel combination of two approaches, namely, an *in vitro* iteration procedure, known as systematic evolution of ligands by exponential enrichment (SELEX), to select aptamers from a combinatorial RNA library, and a laser-pulse photolysis technique with a microsecond time resolution to screen the putative RNA aptamers against the *functional* forms (i.e., non-desensitized) of the receptors. As I have described in the proposal, GluR2, a key AMPA receptor subunit in mediating excitotoxicity, has been chosen to be the target of aptamer selection and thus the target of action to control the excitotoxicity. To test this hypothesis, I have proposed three Tasks, described below.

In Task 1, high affinity RNA aptamers that target GluR2 AMPA receptors will be selected from an RNA library consisting of ~10^{13} sequences using SELEX. Three AMPA receptor inhibitors (NBQX, philanthotoxin-343 and GYKI 47261) were proposed to displace RNAs previously bound to the receptor sites. By our design, two types of aptamers, competitive (using NBQX, a classic competitive antagonist) and noncompetitive (using philanthotoxin and GYKI inhibitor), are expected. This is because RNA molecules bound to the same site and/or to site mutually exclusive as a compound listed above are eluted during the selection.

In Task 2, each of the four AMPA receptor subunits, i.e., GluR1 to GluR4, will be expressed in HEK-293 cells. The channel opening kinetics of the homomeric channel will be characterized using the laser-pulse photolysis and caged glutamate. The channel-opening and the channel-closing rate constants as well as the dissociation equilibrium constant for glutamate will be determined. Likewise, two representative kainate receptor subunits, GluR5Q and GluR6Q, both of which can form the corresponding homomeric receptor channel respectively, will be characterized.

In Task 3, the affinity of an aptamer for both the closed and open forms of a homomeric AMPA receptor channel will be measured. The selectivity of each aptamer for all AMPA receptor subunits will also be determined. The use of the kainate receptors ensures that the desired aptamers will be selective to AMPA receptors, while the use of individual AMPA receptors further ensures that subunit-specific aptamers within the AMPA receptor subtype will be identified.

The significance of this research is as follows. First, an aptamer is different from a chemically synthesized compound in that an aptamer is a single-stranded nucleic acid in nature. The inhibitory property of the aptamer is its uniquely folded three-dimensional structure that confers a high affinity. Second, aptamers are RNA molecules so that they are naturally water soluble. Third, the use of SELEX (see Fig. 1 below) to evolve aptamers does not require the knowledge of the structure of the target protein. This is especially advantageous because glutamate receptors, including GluR2 AMPA receptor subunit, are all membrane proteins and the holo-receptor structures have not been solved. Fourth, the laser-pulse photolysis technique we developed is a unique kinetic tool capable of investigating the mechanism of action of these aptamers against the $GluR2Q_{flip}$ open-

channel conformation that exists less than a few milliseconds after binding of glutamate. The study of this kind has not been previously possible.

2. BODY

Before I describe the research progress, I wish to note that this grant has been recently approved for a no-cost extension for one year so that we can continue our project. Therefore, this progress report represents an annual report covering the progress we made during the period of December 8, 2007 – December 7, 2008.

First, I wish to summarize the progress we have made so far. We have successfully selected two major classes of aptamers against the $GluR2Q_{flip}$ AMPA receptor subunit, using SELEX (see Fig. 1). One class is competitive and the other is noncompetitive aptamers. In the second class, we have further selected two different types of noncompetitive aptamers: one is open-channel conformation specific, namely this type prefers to inhibit the open-channel conformation of the GluR2 receptor, whereas the other prefers to inhibit the closed-channel receptor conformation. Based on this result, we have successfully completed Task 1, as originally proposed. Our results of the selection and characterization of the competitive aptamers have been published. The work on characterizing the noncompetitive aptamers is ongoing. I should emphasize that aptamers, as high affinity, water soluble AMPA receptor inhibitors, have never been reported previously. Furthermore, there is no known inhibitor targeting specific AMPA receptor conformations. Therefore, our work not only represents a conceptual advance in development of inhibitors but also materialization of some unique inhibitors ready to be developed into potential therapeutics. Furthermore, we have completed the rapid kinetic investigations of the channel-opening kinetic mechanism for AMPA receptor subunits, or precisely each of the homomeric AMPA receptor channels, namely, GluR1-4, including the flip and flop isoforms. Some of the results have been published already. Based on the progress we have made thus far, I characterize that we have successfully completed the objectives set out in Tasks 1 and 2.

Our work is now focusing on Task 3. In the last Progress Report I submitted, dated on January 7, 2008, which at the time was called the “final progress report”, I had provided a comprehensive description of our accomplishment up to that time. However, that report also provided a detailed description of the methods we developed and used. In this progress report, therefore, I would like to focus on the accomplishments we have made in the last year, including several key discoveries in our work, which I will describe below. These exciting discoveries have provided us with exciting ideas, which has allowed us to establish several key collaborations to pursue these ideas towards developing a potential ALS therapy.

2.1. Methods

I wish to first describe the two main approaches we used, which are crucial to our success in research.

2.1.1. Selection of Aptamers as Inhibitors Using SELEX

The first main approach is SELEX. The principle and the experimental procedure of using SELEX for aptamer discovery have been described in detail in my proposal and are illustrated in Fig. 1 below (2, 3). As shown, an RNA library was mixed with the $GluR2Q_{flip}$ AMPA receptors expressed in HEK-293 cells (this is the binding step). Then, a chemical inhibitor, such as NBQX, was used to elute competitive aptamers bound to the same site and/or different site(s) that were mutually exclusive (i.e., NBQX or 1,2,3,4-tetrahydro-6-nitro-2,3-dioxo-benzol[f]quinoxaline-7-sulfonamide disodium is a classic competitive inhibitor for AMPA receptor). The eluted RNA molecules were reverse-transcribed and PCR-amplified. The new, enriched pool of RNAs was made by *in vitro* transcription. The new RNA pool was used for a new round of selection. After about 14 rounds of selections, the SELEX was terminated. The DNA pool from the 11th, 12th and 14th rounds were cloned and sequenced. Consensus sequences were then identified by sequence alignment.

I should also mention that although the chemical pressure drawn in Fig. 1 is NBQX, an elutant used to select competitive inhibitors, we have also used two 2,3-benzodiazepine compounds, also known as GYKI compounds, and successfully selected two classes of noncompetitive inhibitors, which I will describe in detail in Section 2.2. Like I have described in my previous reports, we developed methods necessary to carry out SELEX with ion channels like glutamate receptors transiently expressed in HEK-293 cells. Again, our success

of using SELEX to evolve aptamers against a recombinant ion channel protein expressed in heterologous expression system such as in HEK-293 cell line, is the first of this kind.

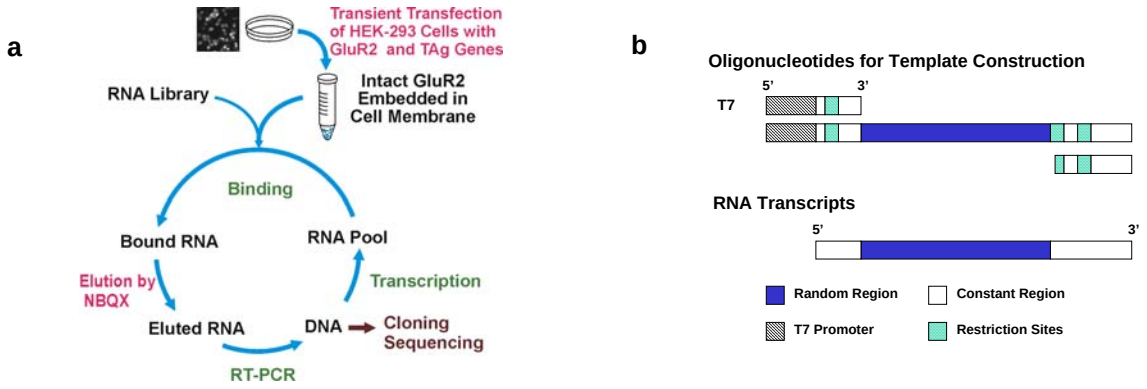

Fig. 1. (**a**) SELEX flow chart. The library we used for SELEX contains a sequence degeneracy of ~10^{15}. The DNA template contains 118 nucleotides. (**b**) The combinatorial RNA library is made by transcribing the DNA templates. Each template consists of 108 bases with a 40-base randomized segment. This segment is flanked by two constant regions for primer annealing. The 5' constant sequence includes a promoter for T7 RNA polymerase. The two restriction sites are E*coRI* located in the 5' constant region and H*indIII* located in the 3' constant region, respectively.

2.1.2. Measuring the Glutamate Receptor Channel-opening Kinetics Using Laser-Pulse Photolysis Technique

An AMPA receptor opens its channel in the microsecond (μs) time scale and desensitizes within a few milliseconds (ms) in the continued presence of glutamate. Competitive and noncompetitive inhibitors are presumed to interact with the channels within this time domain. However, as one of the most commonly used techniques, equilibrium binding using radioligand is relevant to the desensitized receptors in general. Single channel recording can measure rapid kinetics, but has not worked well with AMPA and kainate receptors, because of an intrinsic short lifetime or a rapid channel closing rate constant. Therefore, the mechanism of inhibitor-receptor interactions within μs-to- ms time scale is poorly understood, due to the fact that the time resolution of the conventional kinetic assays is not sufficient to measure the channel opening kinetics of the AMPA and kainate receptor channels.

The laser-pulse photolysis technique using caged neurotransmitters has been developed to measure the receptor channel opening kinetics and inhibitor-receptor interaction with a μs time resolution (4, 5). Caged neurotransmitters are biologically inert, but photolabile precursors of neurotransmitters. This technique utilizes a rapid photolytic release of a neurotransmitter from the caged precursor within the μs time domain to overcome

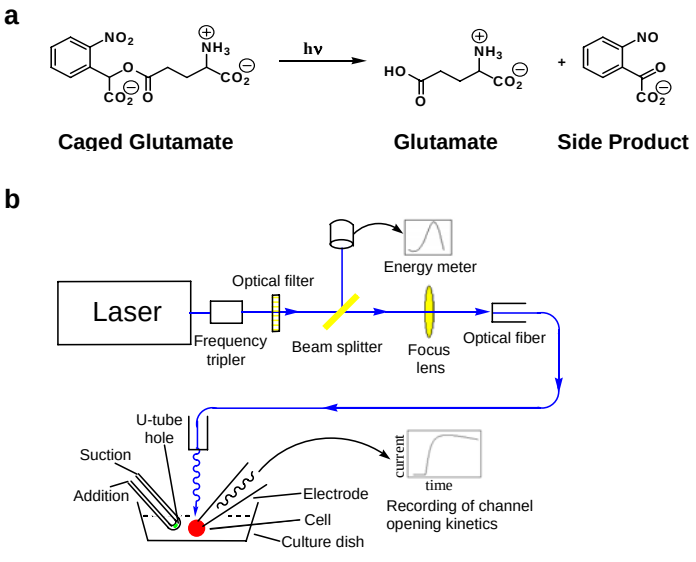

Fig. 2 (a) Photolysis of the caged glutamate. (b) Schematic drawing of the laser-pulse photolysis setup and a U-tube device for delivering caged neurotransmitters (and also free neurotransmitters and inhibitors) to the surface of a cell. The U-tube device, shown in the left, is made from stainless steel tubing with its hole of 150 μm facing towards right. The addition of the solution containing the ligand and the suction of the waste are controlled by two peristaltic pumps. A HEK-293 cell (~15 μm in diameter) is suspended from the recording electrode and placed ~100 μm away from the hole. The linear flow rate of the solution is 1-4 cm/s. An optical fiber through which laser light for photolysis is delivered to the cell has a core diameter of 300 μm. The distance between the cell and the fiber is ~400 μm. The photolysis of caged glutamate liberates free glutamate, which activates the glutamate receptors, and the whole-cell response is recorded.

otherwise a slow diffusion and mixing of free neurotransmitters with the receptor on the surface of a cell. Using this technique, the opening of a receptor channel can be measured prior to receptor desensitization (6). To study glutamate receptors, we have synthesized a caged glutamate (4). The structure of the caged glutamate and the set-up of the laser-pulse photolysis technique are shown in Fig. 2. These two methods or techniques, described above, are the primary approaches we have used in the proposal research.

Next I wish to describe the specific accomplishments in the past year, which I shall divide into different categories for the clarity of presentation. The relationship of these results with the specific Tasks outlined in my original proposal will be also noted.

2.2. Aptamer Characterization

2.2.1. Summary of the work prior to December 7, 2007

Our first project in using SELEX to evolve aptamers against GluR2 AMPA receptors was with NBQX, a classical competitive inhibitor, so that we aimed to identify competitive aptamers. I have provided the rationale and the data in previous reports for this SELEX, and we have already published this work. I should also mention that the competitive aptamers we have selected, most notably the AN58 aptamer (7), are unique inhibitor templates for drug development. They are water soluble and highly potent, rivaling any existing small, organic compounds. Judged by the IC_{50} value, AN58 is the most potent AMPA receptor inhibitors ever reported thus far.

In my last report, I described in detail the selection of the two groups of noncompetitive aptamers. In the past year, we then focused on characterizing the inhibitory properties of these aptamers. I should also mention that one group of noncompetitive aptamers is open-channel conformation specific, namely this type prefers to inhibit the open-channel conformation of the GluR2 receptor, whereas the other group prefers to inhibit the closed-channel receptor conformation. Developing conformation-specific inhibitors, such as those noncompetitive types of aptamers, using SELEX is a novel concept. Therefore, our results show a promising methodology in discovering potential inhibitors with such properties. Furthermore, we now have in fact real molecules or aptamers in hand for future drug development.

2.2.2. Characterization of Noncompetitive Aptamers Using GYKI Compounds

GYKI compounds are 2,3-benzodiazepine derivatives and are one of the most popular inhibitors developed for AMPA receptors. GYKI compounds are thought to be noncompetitive inhibitors. I proposed to use these compounds to elute aptamers that are either bound to the same site(s) or a mutually exclusive site(s). Therefore the aptamers selected are putative noncompetitive inhibitors, based on the principle of SELEX, which we demonstrated using NBQX as described. The noncompetitive nature of these GYKI compounds was established based on radioligand binding studies previously (8) and our mechanistic investigation using the laser-pulse photolysis technique, which I shall describe later in this report.

Using the method we have worked out by the initial selection of competitive aptamers, we further carried out SELEX procedures using two different GYKI compounds whose chemical structures are shown in Fig. 3. Specifically, Cf is a noncompetitive inhibitor, and its inhibition constant for the closed-channel form of

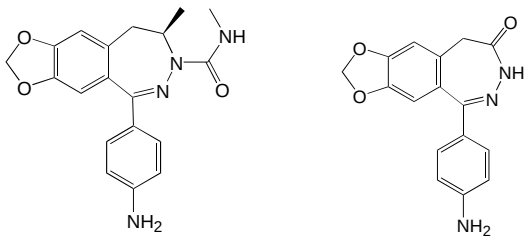

Cf BDZ-2

Fig. 3. Chemical structures of Cf (GYKI 53784) and BDZ-2. Both are the derivatives of the original compound GYKI 52466 [1-(4-aminophenyl)-4-methyl-7,8-methylenedioxy-5*H*-2,3-benzodiazepine] discovered in 1980s (1). For the simplicity of presentation, we named these compounds as Cf and BDZ-2.

the GluR2Q$_{flip}$ receptor or a K_I = 1 μM is six times smaller than for the open-channel form. In contrast, BDZ-2 is a noncompetitive inhibitor with a six-fold higher affinity or a K_I = 6 μM for the open-channel conformation than for the closed-channel form. Again, the method that we used to determine these constants will be described later in this report. We have completed the screening of the aptamers we selected using BDZ-2, and also those we selected using Cf. Among the former group, one aptamer showed a preference of inhibiting the open-channel conformation, as expected (Fig. 4). Aptamers selected using Cf have also shown the preference for the closed-channel state. Furthermore, our preliminary studies of these aptamers with the GluR2Q$_{flip}$ receptor channels expressed in HEK-293 cells show that both types of aptamers have apparent K_I values in 300-600 nM. Based on these values, these RNA aptamers have higher affinity than their chemical counterparts used for elution and are a group of noncompetitive inhibitors with the highest potency against AMPA receptors, compared with those published in literature.

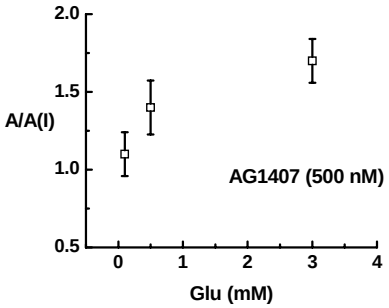

Fig. 4. The ratio of the current amplitude in the absence, *A*, and presence, A_I, of AG1407, an aptamer selected using BDZ-2 (see its chemical structure in Fig. 4 and the inhibitory properties of BDZ-2 in the text and also in *2.5 mechanism of action of GYKI inhibitors.* The current was recorded at 0.1, 0.5 and 3 mM glutamate concentrations with the GluR2Q$_{flip}$ receptor expressed in HEK-293 cells. The glutamate concentration at 0.1 mM and 3 mM correspond to the closed-channel and open-channel receptor forms. As seen, this aptamer is essentially an open-channel preferred inhibitor.

2.2.3. Identification of the Minimal, Functional Sequence Length for Noncompetitive Aptamers

In my last report, I described two objectives of our work in characterizing the noncompetitive aptamers; one was to (a) find out the minimal length of sequence for an aptamer and (b) the other was to test the aptamer with the minimal sequence with all of AMPA receptors and kainate receptor subunits as well as native NMDA receptors endogenously expressed in hippocampal neurons. To date, we have completed (a) or we have identified the minimal, functional sequence for these noncompetitive aptamers. Below I wish to use one example to show the result of this work.

Shown in Fig. 5 is the result of sequence reduction and functional test of the shortened aptamers by the use of whole-cell recording with GluR2 AMPA receptors expressed in HEK-293 cells. In this display or Fig. 5, AF100 represents the full length of an aptamer we have selected, which is a closed-channel preferred noncompetitive inhibitor against GluR2 AMPA receptors.

Fig. 5a **b**

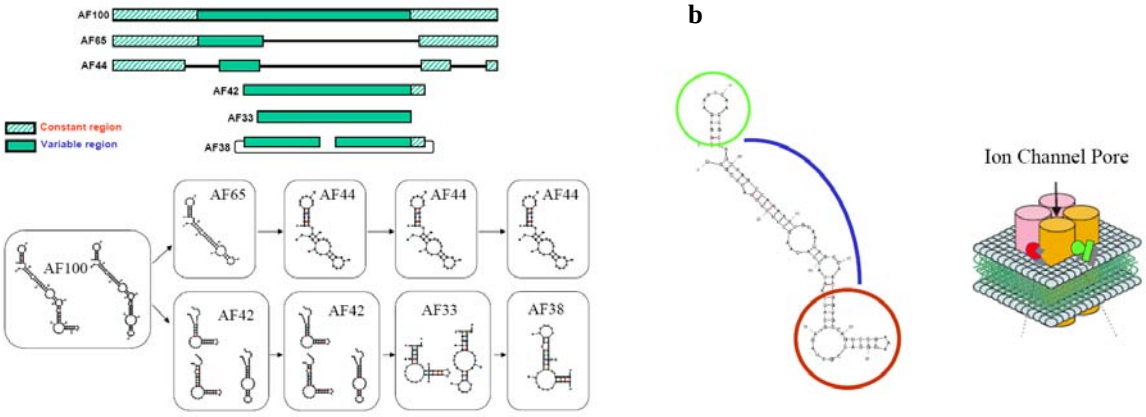

Interestingly, the sequence reduction/functional testing showed that AF100 can be segmentally reduced but not sequentially in that removal of any sequences from either 5′ or 3′ ends of this aptamer led to the loss of the inhibitory function. Yet, AF44 works, provided it is mixed with a second piece, identified as AF42. In other words, the pair of AF44 and AF42 represents the minimal, functional sequence as an inhibitor. Making any more reduction in either piece caused the function. The result suggests that the AF100 encodes both pieces, but the two parts of this aptamers presumably bind alone but act together in order to inhibit the receptor.

Besides being a potential template for drug development, the two functional modules that exist in this aptamer or AF100, as shown in Fig. 5a and depicted in Fig. 5b (the two colored circles), may be also useful potentially as a molecular ruler. An AMPA receptor is considered a “dimer of dimers”, suggesting that there must be at least two topologically different interfaces (as shown, one being brown-brown and the other being pink-brown interface), for instance, for the inhibitor to bind (please note that this consideration is just one of the possible ways that two inhibitory sites could be formed to accommodate two different parts of an inhibitor or an inhibitor pair). If so, making a minimal link using another piece of RNA (like a long based-paired stem) would be able to reveal the distance between the two binding sites. This future study would be significant, because there is no information about the locations and the number of the noncompetitive binding sites in any of the AMPA receptors.

In contrast, AG1407, which is another noncompetitive aptamer and inhibits the open-channel conformation only, has been identified to have the minimal length of 43 nucleotide or 43-nt. Unlike AF100 described above, AG43 was found by a sequential reduction from the 3´ end of the original aptamer length, i.e., 100-nt. The 5´ end of the original aptamer was found to be indispensible.

I should also mention that the sequence reduction and functional testing for every version of the shortened pieces is a labor intensive effort. In the case of AF44 and AF42 pair, deduced from the original AF100, the work was even more since there were two pieces to be tested to decide on the functional pair.

2.2.4. Future Work

The next phase of this project is to test these minimized aptamers with the rest of the AMPA receptors and the kainate receptor subunits as well as native NMDA receptors. Towards that end, we have acquired a plasmid to express GluR5 kainate receptor, from Prof. Peter Seeburg’s group from Germany. This will give us the ability to test an aptamer to see if it has undesirable side activity against the kainate receptors, besides GluR6 kainate receptor subunit. We have acquired the plasmid from Prof. Peter Seeburg’s group from Germany. We have already finished the characterization of this kainate receptor for its dose-response curve. The laser-pulse photolysis measurement for the channel-opening mechanism will follow in the near future. Second, we also plan to test NR1/NR2A, and NR1/NR2B NMDA receptors (NR1, NR2A and NR2B are three different NMDA receptor subunits and none of them alone can form functional channels; yet the two different combinations represent the two most dominant NMDA receptor channels *in vivo*). The ideal outcome through this selectivity assays is to establish that the selected AMPA receptor aptamers would inhibit GluR2 with the highest potency among AMPA receptors, but without any cross activity with either kainate or NMDA receptors.

I should also mention that because the NR1/NR2A and NR1/NR2B are two primary NMDA receptor channel types *in vivo*, the use of these two heteromeric channel types would be sufficient to represent NMDA receptors and at the same time to eliminate the need to use rat hippocampal neurons; therefore, we no longer need to use the animal. We have already received the plasmids of NR1, NR2A and NR2B from Dr. John Woodward at Medical University of South Carolina. We wish to begin the test of aptamers shortly.

2.3. AMPA and Kainate Receptor Channel-Opening Mechanism

2.3.1. Channel Opening Rate Constants

The importance of knowing the rate constants of the channel opening cannot be overemphasized. The rate at which a ligand-gated ion channel opens is important to know, because it has major implications in signal transmission and regulation. First, knowing the constants of the channel-opening rate will allow us to predict more quantitatively the time course of the open-channel form of the receptor as a function of neurotransmitter or ligand concentration, which determines the transmembrane voltage change and in turn controls synaptic neurotransmission. Second, that knowledge will provide clues for mechanism-based design of compounds to regulate receptor function more effectively. This is the subject we are especially interested in for the proposed research because, as I shall demonstrate later in this proposal, understanding how an inhibitor or aptamer affects the channel-opening mechanism is essential in designing better inhibitors and aptamers, and using them more effectively as potential drugs. For instance, a competitive inhibitor will no longer be effective at a saturating

Table 1: Summary of k_{op} and k_{cl} at n =2 for the flip and flop variants of GluR1, 2, and 3 AMPA Receptors

AMPA	k_{op} ($\times 10^4$ s^{-1})	k_{cl} ($\times 10^3$ s^{-1})	K_1 (mM)	R^2
$GluR1_{flop}$	2.7 ± 0.2	2.2 ± 0.2	0.5 ± 0.1	0.96
$GluR1_{flip}$	2.6 ± 0.1	2.2 ± 0.1	0.5 ± 0.1	0.97
$GluR2Q_{flop}$	8.6 ± 0.4	3.7 ± 0.1	1.1 ± 0.1	0.98
$GluR2Q_{flip}$	8.7 ± 0.8	2.6 ± 0.1	1.3 ± 0.1	0.91
$GluR3_{flop}$	9.9 ± 0.5	3.8 ± 0.1	1.0 ± 0.7	0.97
$GluR3_{flip}$	9.6 ± 1.1	1.1 ± 0.2	1.0 ± 0.7	0.91

concentration of an agonist. Third, characterizing the effect of structural variations on the rate constants of channel opening will offer a test of the function, which is relevant to the time scale on which the receptor is in the open-channel form, rather than in the inactive, desensitized form, i.e., ligand-bound, but channel-closed form. Examples of potential structural variations include those due to RNA editing and splicing, and site-specific mutations for investigating the structure-function relationship. Finally, knowing the channel-opening rate constants will be required to understand quantitatively the integration of nerve impulses that arrive at a chemical synapse or that originate from the same synapse but from different receptors responding to the same chemical signals, such as glutamate.

As proposed in Task 2, we have thus far systematically carried out studies of AMPA and kainate receptors for their channel-opening mechanism and have in fact already published on the flip isoforms of every single AMPA receptor subunit, i.e., GluR1-4 (in addition to the flop isoform of GluR3 and the GluR6 kainate receptors). We have also completed the study of the flop isoform of the AMPA receptors. Below, Table 1 is a summary of the flop data we have thus far obtained; the GluR3 flop data were already published and we have another manuscript summarizing the GluR1 flop and GluR2Q flop being reviewed for the revision.

I wish to describe the important finding for our work on characterizing the flop version of the AMPA receptors. In particular, we found that the flop version of GluR2Q responds differently to a GYKI compound as compared to the flip variant of GluR2Q. Therefore, we suspected that the flip/flop site (see Fig. 6) may be involved in formation of noncompetitive sites (we have also additional supportive evidence by NMR studies). This would be an important question to address for noncompetitive aptamers which we are developing. In addition, we found that a flop variant has roughly a 3-fold larger k_{cl} than the flip counterpart (the GluR1 is an exception in that the flip and flop variants have identical k_{cl}, k_{op} and desensitization rate constants). Interestingly, in the spinal cord of ALS patients, the level of the GluR2 flip variant relative to that of the flop isoform on motor neurons is markedly elevated (9). Because the desensitization rate constant of the flip isoform at a given glutamate concentration is ~3-5-fold slower than that of the flop isoform (10), the relative increase of the flip isoform consequently widens the time window for more Ca^{2+} entry, thus rendering the motor neurons more vulnerable to Ca^{2+} insult (9). Thus our data suggest that the flip forms are a very important target of drug development.

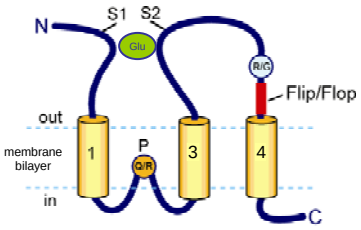

Fig. 6. Topology of an AMPA receptor subunit.

2.3.2. AMPA Channels Desensitize Through the Closed-Channel State and the Channel-Closing Rate Process Regulates the Channel Desensitization

As shown in Table 1, our study of the flip/flop pairs of GluR1 and GluR2, together with GluR3 which we published before (6), shows that the alternatively spliced, flip/flop sequence cassette differentially affects the channel-opening kinetic process of AMPA receptors. The flop sequence of GluR2 correlates to a channel that closes faster than its flip counterpart, without affecting the rate of opening the channel in response to binding of glutamate. Yet for GluR1, the flip/flop sequence cassette does not affect either the channel-opening or the channel-closing rate process. Together, these results implicate possible roles of alternative splicing in both channel gating and the structure-function relationship of the AMPA receptors.

The functional roles we refer to can be realized by comparison of the magnitudes of k_{op} and k_{cl} for various receptor subunits and isoforms. First, the magnitudes of k_{op} and k_{cl} establish quantitatively how fast the channel opens, following the binding of agonist, and how quickly the open channel closes, which is a measure of the lifetime of the open channel or τ, since $k_{cl} = 1/\tau$ (11). For GluR2, the k_{op} for the flop variant is identical, within experimental errors, to that of the flip counterpart (see Table 1). In contrast, k_{cl} of $(3.7 \pm 0.1) \times 10^3$ s^{-1} of the flop variant is ~1.5-fold larger than that of $(2.6 \pm 0.1) \times 10^3$ s^{-1} for the flip (12), suggesting that the open channel of the flop closes ~1.5-fold faster. Therefore, the alternative splicing in GluR2, reflected by a difference of 9 amino acids in the flip/flop sequence cassette affects the channel-opening kinetic properties of these variants by regulating how quickly the open channel closes.

Because the flip/flop sequence cassette in GluR2, like the GluR3 flip/flop pair, affects the channel-closing rate constant or the lifetime of the open channel, it is possible that the flip/flop sequence cassette has a significant structural role in stabilizing the open-channel conformation (6). The presumptive structural role of the flip/flop sequence cassette may be linked to its unique location, in the overall receptor topology, as the flip/flop sequence precedes the putative fourth transmembrane (see Fig. 6). Therefore, it is possible that the flip/flop sequence cassette provides an important structural link of the extracellular ligand binding domain to the membrane-embedded M4 domain, and is therefore involved in stabilizing the extracellular domain, when bound with glutamate, so that the sequence cassette is able to influence the stability of the open-channel conformation (13, 14).

Therefore, we hypothesize the channel-closing rate process kinetically regulates the desensitization reaction in that the faster the open channel closes, the faster the channel desensitizes (15). By this hypothesis, desensitization begins in parallel to the channel-opening reaction, but proceeds, with a slower rate, from the closed-channel state, once glutamate is bound (15). Experimentally, it is without exception that the rate of channel closing in all of the AMPA receptors we have characterized is markedly faster than the rate of channel desensitization at a given concentration of glutamate (6, 11, 12, 16). Thus, our hypothesis represents a simple model that can adequately describe channel desensitization through the closed-channel state, which is kinetically controlled by the lifetime of the open-channel state, and our model does not require that the channel enters the desensitization reaction from the open-channel state. For instance, the flop isoform of GluR2 closes its channel to return to its closed-channel state more quickly than the flip isoform; consequently, the flop channel desensitizes more quickly than the flip isoform. In contrast, the k_{cl} value of the GluR1 flip and flop isoforms are identical, so is the rate of channel desensitization for both isoforms. In addition, a GluR1 mutant with a leucine-to-tyrosine substitution mutation (i.e., $GluR1_{flip}$ L497Y) abolished the tendency of channel desensitization, and, as we found, this mutant had an extremely slow rate of channel closing.

Furthermore, our model links the k_{cl} value as a measure of the stability of the open-channel conformation, and thus predicts that any mutation made anywhere in the receptor affects the channel desensitization if it affects the k_{cl} or the stability of the open-channel conformation.

The conclusions drawn from this work has allowed us to provide new mechanistic insights into the structure-function relationship for the glutamate receptor. The hypothesis we put forth is the direct result of using our rapid kinetic technique, i.e., the laser-pulse photolysis technique, to determining the k_{op} and k_{cl} values for the AMPA receptors, as proposed in Task 2.

2.4. RNA Structure and Function

In the course of the initial work in identifying competitive aptamers, we found a unique RNA aptamer. The same sequence of this RNA aptamer can fold into two structures during, not after, the T7 RNA polymerase-catalyzed transcription reaction. Interestingly, neither structure alone is inhibitory but together as a pair, they are a very potent competitive inhibitor.

More importantly, the two structures, which we termed as M1 and M2 (see Fig. 7), are incapable of interconverting through unfolding (denaturation) and refolding (renaturation) procedures, presumably due to their extraordinary structural stability (see Fig. 7). These results suggest that M1 and M2 are not the folding products of each other. To date, no report has ever appeared that a RNA conformer cannot be reversibly unfolded and refolded. There is not a precedent demonstrating that the two RNA structures assumed from the

same sequence are not reversibly convertible by denaturing and refolding. The conventional view is that an RNA molecule, like a biopolymer, is supposed to be unfolded from a conformation, and upon refolding, folds into different conformations that are in equilibrium among all possible conformations. Clearly, our results show a novel property in RNA structure and function.

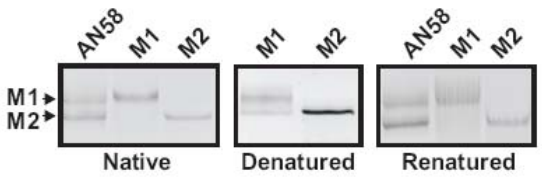

Fig. 7. Unfolding and refolding of M1 and M2. The left panel shows the different mobility of purified M1 and M2 in a native PAGE (10%), compared with the mixture of the original sample, AN58. When the purified M1 and M2 dissolved in the Loading Buffer II (Ambion) for denaturing PAGE, which contained 47.5% formamide, were boiled for 15 min and run in the denaturing PAGE (10%, 7 M urea), additional band appeared originating from the M1 sample (middle panel). The "denatured" M1 and M2 were then precipitated in ethanol and re-suspended in the external buffer; the refolded samples were visualized in another native PAGE (10%) (right panel). In the same native PAGE, the AN58 sample was treated by the same unfolding/refolding process. M1 and M2 used in the folding/refolding experiments were also purified to remove the contaminated polyacrylamide (7).

The significance of our finding is that an RNA can directly carry structural information, in addition to carrying sequence information, because it encodes two structures (not two different conformations). Therefore, our findings provide profound implications in the evolution and folding of RNA structure in nature. For instance, the transfer of *sequence information* between two different classes of nucleic acids is not considered difficult because such a process uses the one-to-one correspondence of Watson-Crick pairing. In contrast, the transfer of *function* is considered difficult because a function is a property of a macromolecule that is inherently more complex than sequence. In a recent study, it was shown that the evolutionary conversion of a ribozyme (RNA) to a deoxribozyme (DNA) of the same function can be accomplished but only with some critical sequence mutations (17). Our finding that the survival of one genotype ensures more than one phenotype through *in vitro* evolution demonstrates that the transfer of different functions through the same sequence in a sequential fashion from DNA to RNA as in our case is possible. Therefore RNA may be more phenotyptically adaptable than proteins. Currently, no protein sequence is known to assume two different folds endowing two functions (18). The results from our study suggest a possibility that in a real organism a single RNA sequence could evolve to "duplicate" RNA molecules with structure-dependent functional dissimilarities, which, in some cases, may precede gene duplication.

I should emphasize that this work was completely a serendipitous discovery based on our work in the selection of aptamers against the GluR2 AMPA receptor using SELEX, as proposed in Task 1. However, because of this profound significance, we have pursued the study of the structure-function relationship of this sequence. Shown below is an example of our studies.

We performed the experiment known as selective 2′-hydroxyl acylation analyzed by primer extension (SHAPE) to probe the conformational dynamics of the structure for M1, M2 and SynAN58 (SynAN58 is the RNA carrying the same sequence as M1 and M2 do, but it is a synthetically made RNA, whereas M1 and M2 are products of the T7 RNA polymerase-catalyzed transcription reaction). Generally in an SHAPE experiment, *N*-methylisatoic anhydride (NMIA) is used, and has been used in our experiment, to react with the 2′-hydroxyl group of a ribose, generating a corresponding ester adduct (see Fig. 8).

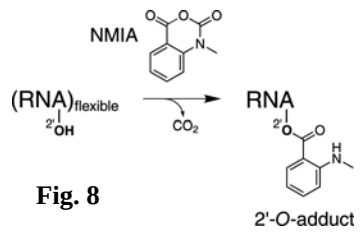

Fig. 8

The acylation reactivity using NMIA in the SHAPE experiment is influenced by the local structure of an RNA such that a flexible nucleotide reacts with NMIA more readily than a nucleotide constrained by either base pairing or a tertiary interaction (19). Thus, the reactivity of the acylation with NMIA can be used to reveal the locations of those conformationally dynamic nucleotides, since the formation of a 2′-ester adduct causes RT pausing in primer extension experiment (19). Shown in Fig. 9a is the gel electrophoresis analysis of the reactivity of NMIA at single nucleotide position up to nucleotide 43 (whereas the last 15 nucleotides in the 58-nt RNA were covered by the primer annealing). From the intensities of bands in the gels, which were quantified for each species using SAFA program, the SHAPE reactivity was calculated (20) (Fig. 9b).

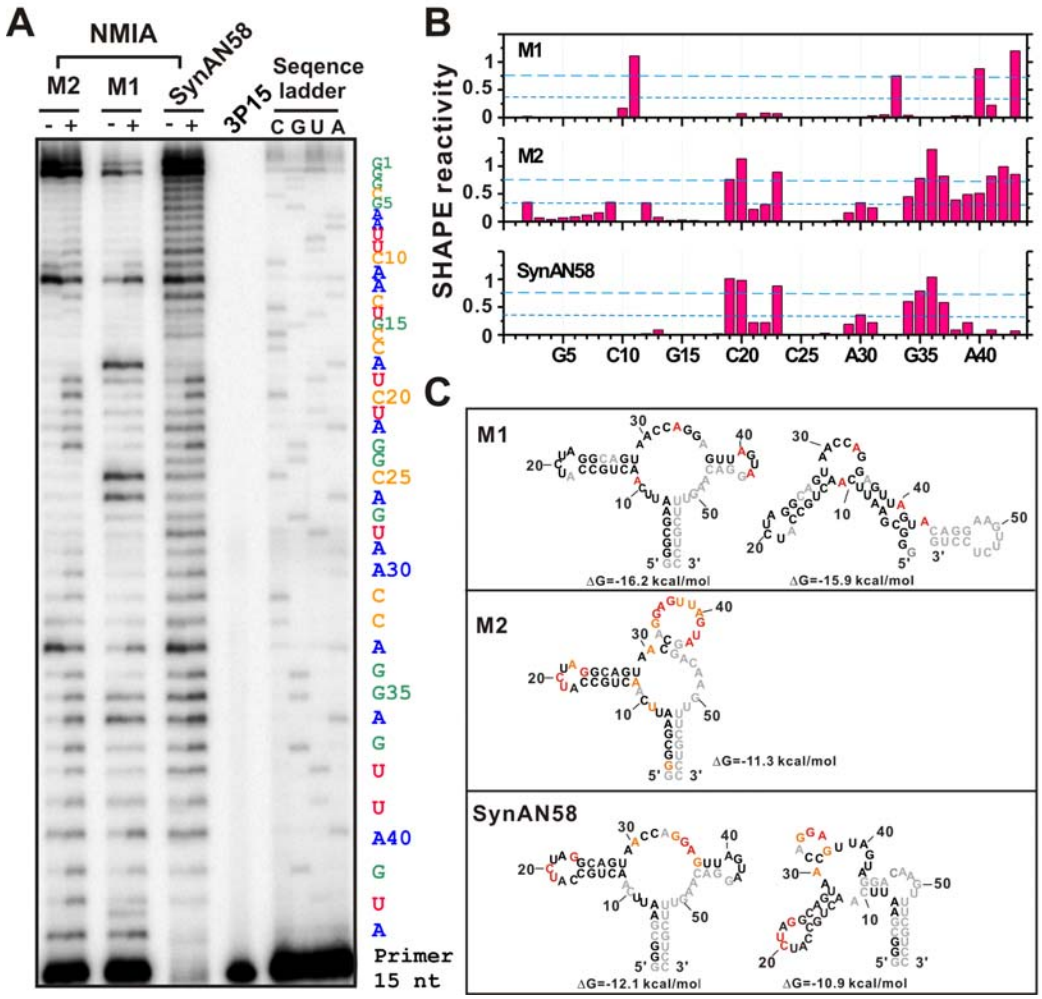

Figure 9. SHAPE analysis of M1, M2 and SynAN58. (**A**) The pattern of NMIA reactivity was probed by a reverse transcription reaction using a 5´-end, 15-nt oligo or 3P15, and visualized on a 12% denatured PAGE containing 8 M urea. Other parameters were described in Materials and Methods. The sequencing ladder, shown on the right, was generated by dideoxy nucleotide incorporation during the primer extension, similar to Figure 2B. (**B**) Band intensity of the SHAPE experiment in the presence and absence of NMIA was quantified by using SAFA software (21). For each nucleotide position, the reactivity was calculated as the intensity difference between the NMIA labeled lane and the negative control lane (i.e., the negative control contained the same concentration of DMSO, the solvent for NMIA). There were also nucleotide positions where no reactivity could be detected or a negative reactivity was detected, due to strong RT stops in the absence of NMIA (Figure 2A). These positions, along with the last 15 nucleotides for primer annealing, all marked in light gray in Figure 3C, were set to be zero in the reactivity value. The SHAPE reactivity score was calculated based on a method described previously (20, 22). The long-dashed blue line indicates the threshold or 0.75 SHAPE reactivity score whereas the short-dashed line represents the threshold of 0.35 SHAPE reactivity score (see text for detailed explanation). (**C**) Secondary structures generated using RNAstructure (version 4.6) (23), based on the SHAPE reactivity score. The number of the structures presented here corresponded to those whose free energy differed by less than 10% of the lowest free energy in each of the RNA structures.

Comparison of the quantitative SHAPE reactivity among M1, M2 and SynAN58 (Fig. 9b) showed that the overall number of nucleotides that were labeled and their respective positions were different, consistent with the notion that each of the three species with the same sequence had a distinct structure. In particular, M1 had the least number of the nucleotide positions labeled overall. Furthermore, in two major segments where both M2 and SynAN58 reacted prominently with NMIA, e.g., U19-G23 and G34-G37, the same nucleotides in M1 exhibited no NMIA reactivity. In general, non-reactive nucleotides were thought to be Watson-Crick based-paired. A number of non-canonical base pairing, such as U-G, A-A and A-G, could also become nonreactive. We therefore concluded that a major network of base pairing and possibly tertiary interactions existed in M1, rendering only a few nucleotide residues flexible or unpaired. This conclusion is entirely consistent with result

from the in-line probing experiment with M1 (data not shown), where a large portion of its structure showed considerable resistance to degradation on the same time scale, as compared with both M2 and SynAN58.

In contrast, the overall SHAPE reactivity patterns between M2 and SynAN58 were similar (Fig. 9b), suggesting the two were structurally similar. However, there were clear differences. For instance, the SHAPE reactivity terminated at G37 for SynAN58, whereas it continued from U38-A43 for M2. This result indicated that the 3′ region may be the location that distinguishes M2 from SynAN58. Consistent with this result, the in-line probing experiment we preformed (data not shown) showed that M2 and SynAN58 had key structural difference in G55-C57 at the 3′ end (these three nucleotides were not detectable in SHAPE experiment because they were part of the primer annealing site). It is further worth noting that in between U38-A43, SynAN58 showed no SHAPE reactivity, while M1 was labeled but only at A40 and A43, as compared to a broader reactivity in M2. Together, these results highlighted the importance of the 3′ region in defining the unique structures of these species.

Based on both the primary RNA sequence and more importantly, the three sets of SHAPE reactivity scores (Fig. 9b), we predicted the secondary structures (Fig. 9c) for M1, M2 and SynAN58, using an RNA structure prediction algorithm (23). The SHAPE reactivity was especially useful in obtaining a more accurate output of the secondary structure prediction, because these scores provided experimental evidence to constrain the locations of the conformationally dynamic nucleotides (20). However, it should be noted that the following parameters were taken into consideration in structural prediction (20, 22). First, the reactivity score of 0.75 (i.e., the long-dashed line in Fig. 3b and the nucleotides labeled in red in Fig. 9c) corresponded to the threshold of single-stranded, highly reactive nucleotide residues. The reactivity score between 0.75 and 0.35 (i.e., the short dashed-line in Fig. 9b and the nucleotides labeled in orange in Fig. 9c) was considered to be either base-paired or adjacent to bulges, mismatches, or G-U pairs, which could be more dynamic than nucleotides in the center of an uninterrupted helix. For the reactivity score below 0.35, the nucleotides were considered base-paired (20, 22). Based on these SHAPE reactivity constraints, the secondary structures generated for M1, M2 and SynAN58 were clearly different (Fig. 9c). For instance, in the constant region of the RNA aptamer or nucleotides of G1-C25 (7), a stem-loop was predicted (Fig. 3c), supported by the labeling of some nucleotides by NMIA in both M2 and SynAN58. However, the lack of NMIA reactivity in M1 roughly in the same loop position suggested that M1 may have a more complex structure in this region such that the loop participated in a tertiary interaction. Furthermore, for both M1 and M2, there seemed to be a stem-loop, as indicated by A40. However, such a region showed no SHAPE reactivity for SynAN58 (Fig. 9c). The lack of the SHAPE reactivity near A40 for SynAN58 suggests a conformationally constrained local structure or is indicative of the involvement of this loop in a tertiary interaction.

The results from the SHAPE experiment, which is just an example of our study on this subject, have been consistent with the finding from all of the experiments we have done so far and consistently support that hypothesis that M1 and M2, the two enzymatic products, have different structures, but none is the same as the structure folded by the synthetically made RNA or SynAN58, despite that all share the same sequence.

I should mention that the manuscript summarizing this work has been resubmitted to *Nature*. The earlier version of this manuscript was sent out for external review more than one year and half ago. We have since then been diligently working on this subject to improve the number and the scope of our experiments in order to prove this “extraordinary claim” and “potentially very significant research”, as the reviewers called it.

2.5. Testing Chemically Modified Aptamers

We have successfully demonstrated that RNA aptamers with nanomolar affinity can be successfully selected using SELEX against GluR2, a key AMPA receptor subunit that mediates excitotoxicity. The methodology of discovering inhibitors is different from conventional ones, and the inhibitory properties of these aptamers rival any existing, small molecule inhibitors. Furthermore, we have three different types of aptamers all with nanomolar potency, including some conformation-selective aptamer inhibitors. These RNA aptamers represent novel and promising lead compounds for drug development for an effective ALS therapy. However, translation of aptamers from powerful *in vitro* inhibitors against AMPA receptors “on the bench” into potential ALS therapeutics “to the bedside”, which is the ultimate goal of this research, requires us of making aptamers

suitable to be tested in various settings, such as cellular, animal and humans. These tests are needed to validate the effectiveness and the potency of neuroprotection of AMPA-receptor mediated cell death.

Towards that end, the bioavailability of an aptamer must be improved in terms of increasing its biostability, thereby prolonging systemic exposure of the aptamer. The stability of an RNA molecule in biological fluid containing ribonucleases is determined by its backbone composition. Unmodified, a typical RNA can be degraded *in vivo* at the 2'-OH position by ribonucleases in a half-life of several minutes. The 2'-OH of RNA can attack the 5'→3' intra-phosphodiester bond and cause backbone self-cleavage. Therefore, natural or exogenous unmodified RNA molecules are limited in therapeutic applications by their inherent sensitivity towards ribonucleases *in vivo*. However, changing the 2′-OH group in ribose to 2′-NH_2 or 2'-fluoro (2′-F) modified sugars on pyrimidines, for instance, can be sufficient to make the RNA resistant to nucleases in serum with a half-life of >2 days. Therefore, the starting point of our work towards translating inhibitors into real drugs as our ultimate goal is to make chemically modified aptamers. We believe making chemically modified, yet effective aptamers, is an integral part of Task 3. In fact, the task of making chemically modified aptamers is like a control experiment, because testing these modified aptamers in a cellular model, like motor neurons, is to validate their actual effectiveness as AMPA receptor inhibitors.

To approve that chemical modification is necessary and is a viable approach, we tested our aptamers with and without chemical modification. As seen in Fig. 10, just changing the 2′-OH group to 2′-F on all of the U bases has resulted in a dramatic increase of the lifetime of the RNA aptamer in cerebrospinal fluid (CSF), when compared to the unmodified aptamer (see the legend of Fig. 10). Obviously, additional modifications in other bases would supposedly show additional lengthening of the lifetime of the aptamer.

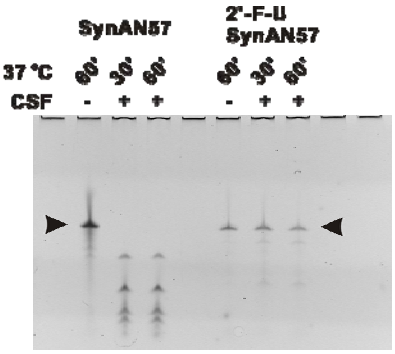

Fig. 10. After quantification, there are roughly 95% and 70% of 2'-F-U modified SynAN57 left after 30 min and 60 min incubation with CSF, respectively. The unmodified or regular SynAN57, 100% of the sample was degraded, appearing as fragmented pieces or multiple low bands, even after 30 min incubation with CSF. AN57 is a modified version of AN58, lacking one A (either A17 or A18), and AN57 is still functionally active. The CSF from rats was kindly provided by Dr. Jacqueline Sagen at School of Medicine at University of Miami (we have a collaboration on another project).

I should mention that I have established collaboration with Dr. Lee Rubin at Harvard Stem Cell Institute whose lab has developed a large-scale production and culturing of mouse embryonic stem (ES) cell-derived motor neurons for high throughput, high content assays to screen drugs that will prolong the survival of the motor neurons. We will test our aptamers in motor neurons, the intended cellular target of these aptamers, since the effectiveness of an inhibitor in motor neuron protection against glutamate-induced cell death is considered one of the most important standards to measure the neuroprotective potential of that inhibitor. Rubin's lab has developed a large-scale production and culturing of mouse embryonic stem (ES) cell-derived motor neurons, including the motor neurons that express G93A human SOD1 gene, for high throughput, high content assays. Therefore, his lab will be able to help us test and screen aptamers that will prolong the survival of the motor neurons. Rubin's lab has generated is equipped with automated cell plating devices (Biomek uFill), Cy-Bi liquid handling systems with cell culture incubators, and a Titertek MapD workstation for fixation (and antibody staining when needed). The toxicity/survival assay will be conducted using a Perkin-Elmer Evotec Opera high throughput confocal microscope. Obviously this will be a future joint effort between my lab and Rubin's lab at Harvard. Making chemically modified aptamers is the first step to make these tests in motor neurons possible.

3. KEY RESEARCH ACCOMPLISHMENTS

- Successfully selected two groups of noncompetitive aptamers; these aptamers show differential affinity towards different receptor conformations, one being the closed-channel and the other being the open-channel conformation. Therefore, we now have a total of three types of aptamers, including a group of competitive aptamers. These studies are the work proposed in Task 1.
- All of the aptamers inhibit the $GluR2Q_{flip}$ receptor, a key AMPA receptor subunit to mediate glutamate-induced neurotoxicity linked to ALS, noncompetitively. The apparent K_I values or IC_{50} values for these aptamers are all in the nanomolar region. Therefore, they are more potent than the chemical counterparts. Based on literature values for those published, small molecule inhibitors, the noncompetitive aptamers we have selected have higher potency than any of the existing inhibitors.
- Completed the sequence reduction and functional testing of the aptamers. Identified two RNA aptamers with the minimal length.
- Completed the measurements of the channel-opening rate constants or k_{op} and k_{cl} for the flop isoforms of GluR1 and GluR2, using the laser-pulse photolysis measurement. Therefore, we have completed a systematic characterization of the kinetic mechanism of the channel opening for 9 receptor channels to date, and they are both the flip and flop variants of the GluR1, GluR2, GluR3 and GluR4 AMPA receptors, and a mutant GluR1 channel (i.e., GluR1L497Y mutant). Furthermore, we have also characterized the rapid kinetic investigation of the GluR6Q kainate receptor. These studies are the work proposed in Task 2.
- We have also carried out a series of rapid kinetic investigations on the mechanism of inhibition for GYKI compounds, which are inhibitors of AMPA receptors and were the ones we have screened and identified; we have successfully used them for the elution and discovery of noncompetitive aptamers. One paper is published and the other is near completion in manuscript preparation. Several of these compounds are being studied in my lab at this moment.
- We have also determined the structure-function relationship for AN58, an aptamer which apparently can form two structures with the same sequence, rather than two different conformations, that cannot be denatured and refolded into other conformation.
- We have also begun to test chemical modifications on aptamers we have selected. We aim to make stable, yet still potent, aptamers suitable to be tested for their neuroprotective potency in cellular models (such as ALS motor neurons).

4. REPORTABLE OUTCOMES

4. 1. Papers and submitted manuscript:

Ritz, M., Micale, N., Grasso, S. and Niu, L. (2008) *Biochemistry* **47**, 1061-1069. A Laser-Pulse Photolysis Study of the Mechanism of Inhibition of the GluR2 AMPA Receptor by 2,3-Benzodiazepine Derivatives

Pei, W.M., Huang, Z., Wang, C., Han, Y., Park, J.S., and Niu, L. (2008) submitted to *Biochemistry*. Flip and Flop: a Molecular Determinant for AMPA Receptor Channel Opening

Huang, Z., Pei, W.M. Jayaseelan, S., Shekhtman, A. Shi, H., and Niu, L. (2008) submitted to *Nature*. One RNA Aptamer Sequence, Two Structures: A Collaborating Pair that Inhibits Glutamate Receptors

4. 2. Four manuscripts are in preparation:

Ritz, M., Micale, N., Grasso, S. and Niu, L. (2008) Mechanism of Inhibition of the GluR2 AMPA Receptor Channel Opening by GYKI 52466

Huang, Z. Han, Y and Niu, L. (2008) Selection of the Open-Channel Conformation-Specific Aptamers against the GluR2 AMPA Receptor

Park, J. S., Huang, Z. Han, Y, Wang, J. and Niu, L. (2008) Selection of the Closed-Channel Conformation-Specific Aptamers against the GluR2 AMPA Receptor

Jayaseelan, S, Huang, Z., Theimer, C, and Niu, L. (2008) Folding and unfolding of three RNA species with the same sequence.

4. 3. Abstracts:

- Poster presentation at the RNA Society Meeting in Berlin, Germany. One RNA Aptamer Sequence, Two Structures: A Collaborating Pair that Inhibits Glutamate Receptors (July 27 -- August 2, 2008).

4. 4. Presentations:

- Invited participation and presentation of our aptamer results in "Accelerating ALS Research: Translating basic discoveries into therapies for ALS", a meeting sponsored by the ALS Association (Jan 13-16, 2008, Tampa, FL).
- Invited presentation at the 26th Regional Meeting on Kinetics and Dynamics. The title of my talk is Mechanism of the inhibition of AMPA receptor channel opening by 2,3-benzodiazepine derivatives (Jan 26, 2008)
- Invited talk at the Chemistry Department, SUNY-Binghamton. Glutamate Receptors, Chemical Kinetics, Inhibitors, and RNA Aptamers (April 11, 2008).
- Invited talk at the Hudson Valley RNA Journal Club: Glutamate Receptor Aptamers (May 21, 2008).
- Invited talk at the Department of Medicinal Chemistry, University of Copenhagen, Denmark. Glutamate inhibitors and aptamers (August 5, 2008)

4. 5. One patent has been filed with USPTO:

Nucleic Acid Ligands Specific for Glutamate Receptors (2004) Li Niu, Zhen Huang, Hua Shi, John T. Lis.

Note that we have received positive court opinions for the initial patent applications. We have made modification based on the required changes on the allowable number of claims.

4. 6. Funding applied for based on work supported by this award:

CURRENT FUNDING

Besides the current funding from DOD, I have obtained an additional funding from MDA.

A Research Grant (PI: Niu) 7/1/08-6/31/09
Muscular Dystrophy Association
Kinetic Studies of GYKI Compounds as Neuroprotective Agents for ALS
This grant funds a small scale study of a few targeted GYKI compounds by kinetic assays, and by cellular and tissue toxicity models to test their neuroprotective properties.
Role: PI

GRANT PENDING FOR FUNDING

RO1 (PI: Niu) 4/1/09-3/30/14
NIH
Mechanistic Studies of GYKI Compounds
This grant proposal concerns rapid kinetic studies of the mechanism of inhibition of AMPA receptors.

GRANTS BEING REVIEWED

Department of Defense (PI: Niu) 1/1/09-12/31/09
Concept grant
Development of GluR6-Selective Aptamers for Potential Autism Therapy
This project is to develop RNA aptamers against a GluR6 kainate receptor mutant thought to be involved in autism.
Role: PI

Department of Defense (PI: Niu) 4/1/09-3/30/14
Advanced Tech./Therapeutic Develop. Grant
Developing Biostable Aptamers for ALS Therapy
This study is to develop RNA aptamers as *in vivo* drug candidates, and to test them in cellular, tissue and animal models for ALS therapy
Role: PI

Department of Defense (PI: Niu) 7/1/09-6/31/11
Idea Award
Discovery of AMPA Receptor Potentiating Aptamers as Cognitive Enhancers
This project is to use SELEX to develop RNA potentiating aptamers that are potential drug candidates for treating memory-deficient and memory disorders involving AMPA receptors
Role: PI

R21 (PI: Niu) 9/1/09-8/30/11
NIH/NINDS
Exploratory/Developmental Projects in Translational Research
Developing Biostable Aptamers
This grant proposal is to evolve chemically modified aptamers using SELEX against AMPA receptors.

5. CONCLUSIONS

Making and using AMPA receptor inhibitors to block excitotoxicity mediated by AMPA receptors currently suffers two major problems. First, the number of existing AMPA inhibitors is limited and so is their water solubility. Second, the inhibitors are generally characterized with the desensitized receptor form(s) because the commonly used methods are either equilibrium binding or conventional kinetic techniques, the latter of which has an insufficient time resolutions to assay the receptor that upon binding glutamate opens its channel in the microsecond time region and begins to desensitize even within a few milliseconds. As a result, the detailed mechanism of action and efficacy of these inhibitors/drugs are poorly understood. These problems have significantly hampered drug development for treatment of ALS.

We have proposed to take a totally different approach, an unconventional one, to develop AMPA receptor inhibitors in that an *in vitro* evolution method, SELEX, has been used to identify RNA inhibitors or aptamers from a RNA library, and the inhibitors themselves are actually RNA molecules. We hypothesized that these RNA aptamers would be found and they would have nanomolar affinity, rivaling their chemical inhibitor counterparts. To date, we have indeed successfully accomplished these objectives or Tasks 1 and 2. Specifically, we have identified two classes of aptamers or competitive and noncompetitive classes, both of which have apparent K_I in the nanomolar region for inhibiting the $GluR2Q_{flip}$ AMPA receptor channels. In the noncompetitive category, we further identified two groups of aptamers specific towards unique receptor conformations.

I should emphasize that aptamers as high affinity, water soluble compounds have never been reported previously. Furthermore, there is no known inhibitor targeting specific AMPA receptor conformations. Therefore, our work not only represents a conceptual advance in development of inhibitors but also

materialization of unique inhibitors or aptamers entirely different from traditional, small molecule inhibitors. We have further demonstrated the feasibility that chemically modified aptamers show promising stability under a physiological condition, and therefore, these aptamers are testable for cellular, tissue and animal models for their effectiveness, potency and potentially toxicity assays towards the ultimate goal of using them as a new therapy for ALS. Currently, we are continuing on characterizing aptamers for their selectivity and possible cross activity, for the noncompetitive aptamers, as we proposed in Task 3. We have made major breakthroughs thus far in our proposed work, and we are extremely excited to continue our work ahead.

I do wish to ask the permission to change the protocol of assaying aptamers against native NMDA receptors. Originally, we planned to use rat hippocampal neurons which express endogenous NMDA receptors. However, that approach requires the use of animal. I propose to test our aptamers with the NR1/NR2A and NR1/NR2B, the two primary NMDA receptor channel types *in vivo*. We can transiently express these channels in HEK-293 cells, as we have done with other glutamate receptor channels. The use of these two heteromeric channel types is sufficient to represent NMDA receptors and, at the same time, to eliminate the need to use rats for harvesting hippocampal neurons. Like I indicated, we have already obtained the plasmids of NR1, NR2A and NR2B from Prof. John Woodward's lab at Medical University of South Carolina. I wish to get the permission so that we can begin our assays shortly.

6. REFERENCES

1. Tarnawa, I., Farkas, S., Berzsenyi, P., Pataki, A., and Andrasi, F. (1989) Electrophysiological studies with a 2,3-benzodiazepine muscle relaxant: GYKI 52466. *Eur J Pharmacol.* **167**, 193-199.
2. Ellington, A. D., and Szostak, J. W. (1990) In vitro selection of RNA molecules that bind specific ligands. *Nature* **346**, 818-822
3. Tuerk, C., and Gold, L. (1990) Systematic evolution of ligands by exponential enrichment: RNA ligands to bacteriophage T4 DNA polymerase. *Science* **249**, 505-510
4. Wieboldt, R., Gee, K. R., Niu, L., Ramesh, D., Carpenter, B. K., and Hess, G. P. (1994) Photolabile precursors of glutamate: synthesis, photochemical properties, and activation of glutamate receptors on a microsecond time scale. *Proc Natl Acad Sci U S A* **91**, 8752-8756
5. Niu, L., and Hess, G. P. (1993) An acetylcholine receptor regulatory site in BC3H1 cells: characterized by laser-pulse photolysis in the microsecond-to-millisecond time region. *Biochemistry* **32**, 3831-3835
6. Pei, W., Huang, Z., and Niu, L. (2007) GluR3 flip and flop: differences in channel opening kinetics. *Biochemistry* **46**, 2027-2036
7. Huang, Z., Pei, W., Jayaseelan, S., Shi, H., and Niu, L. (2007) RNA Aptamers Selected against the GluR2 Glutamate Receptor Channel. *Biochemistry.* **46**, 12648-12655. Epub 12007 Oct 12612.
8. Grasso, S., Micale, N., Zappala, M., Galli, A., Costagli, C., Menniti, F. S., and De Micheli, C. (2003) Characterization of the mechanism of anticonvulsant activity for a selected set of putative AMPA receptor antagonists. *Bioorg Med Chem Lett.* **13**, 443-446.
9. Tomiyama, M., Rodriguez-Puertas, R., Cortes, R., Pazos, A., Palacios, J. M., and Mengod, G. (2002) Flip and flop splice variants of AMPA receptor subunits in the spinal cord of amyotrophic lateral sclerosis. *Synapse* **45**, 245-249.
10. Koike, M., Tsukada, S., Tsuzuki, K., Kijima, H., and Ozawa, S. (2000) Regulation of kinetic properties of GluR2 AMPA receptor channels by alternative splicing. *J Neurosci* **20**, 2166-2174.
11. Li, G., and Niu, L. (2004) How fast does the GluR1Qflip channel open? *J Biol Chem* **279**, 3990-3997. Epub 2003 Nov 3910.
12. Li, G., Pei, W., and Niu, L. (2003) Channel-opening kinetics of GluR2Q(flip) AMPA receptor: a laser-pulse photolysis study. *Biochemistry* **42**, 12358-12366.
13. Armstrong, N., and Gouaux, E. (2000) Mechanisms for activation and antagonism of an AMPA-sensitive glutamate receptor: crystal structures of the GluR2 ligand binding core. *Neuron* **28**, 165-181.
14. Hansen, K. B., Yuan, H., and Traynelis, S. F. (2007) Structural aspects of AMPA receptor activation,

desensitization and deactivation. *Curr Opin Neurobiol.* **17**, 281-288. Epub 2007 Apr 2006.
15. Pei, W., Ritz, M., McCarthy, M., Huang, Z., and Niu, L. (2007) Receptor occupancy and channel-opening kinetics: a study of GLUR1 L497Y AMPA receptor. *J Biol Chem.* **282**, 22731-22736. Epub 22007 Jun 22731.
16. Li, G., Sheng, Z., Huang, Z., and Niu, L. (2005) Kinetic mechanism of channel opening of the GluRDflip AMPA receptor. *Biochemistry* **44**, 5835-5841.
17. Paul, N., Springsteen, G., and Joyce, G. F. (2006) Conversion of a ribozyme to a deoxyribozyme through in vitro evolution. *Chem Biol.* **13**, 329-338.
18. Schultes, E. A., and Bartel, D. P. (2000) One sequence, two ribozymes: implications for the emergence of new ribozyme folds. *Science* **289**, 448-452.
19. Wilkinson, K. A., Merino, E. J., and Weeks, K. M. (2005) RNA SHAPE chemistry reveals nonhierarchical interactions dominate equilibrium structural transitions in tRNA(Asp) transcripts. *J Am Chem Soc.* **127**, 4659-4667.
20. Wilkinson, K. A., Gorelick, R. J., Vasa, S. M., Guex, N., Rein, A., Mathews, D. H., Giddings, M. C., and Weeks, K. M. (2008) High-throughput SHAPE analysis reveals structures in HIV-1 genomic RNA strongly conserved across distinct biological states. *PLoS Biol.* **6**, e96.
21. Das, R., Laederach, A., Pearlman, S. M., Herschlag, D., and Altman, R. B. (2005) SAFA: semi-automated footprinting analysis software for high-throughput quantification of nucleic acid footprinting experiments. *Rna.* **11**, 344-354.
22. Mortimer, S. A., and Weeks, K. M. (2007) A fast-acting reagent for accurate analysis of RNA secondary and tertiary structure by SHAPE chemistry. *J Am Chem Soc.* **129**, 4144-4145. Epub 2007 Mar 4117.
23. Mathews, D. H., Disney, M. D., Childs, J. L., Schroeder, S. J., Zuker, M., and Turner, D. H. (2004) Incorporating chemical modification constraints into a dynamic programming algorithm for prediction of RNA secondary structure. *Proc Natl Acad Sci U S A.* **101**, 7287-7292. Epub 2004 May 7283.

7. APPENDICES

The Appendices include two parts:

(1) The PDF file of the paper by Ritz et al. is attached to this report;
(2) Meeting abstract

Mechanism of Inhibition of the GluR2 AMPA Receptor Channel Opening by 2,3-Benzodiazepine Derivatives†

Mark Ritz,‡ Nicola Micale,§ Silvana Grasso,§ and Li Niu*,‡

Department of Chemistry and Center for Neuroscience Research, University at Albany, State University of New York, Albany, New York 12222, and Dipartimento Farmaco-Chimico, Università di Messina, viale Annunziata, 98168 Messina, Italy

Received April 25, 2007; Revised Manuscript Received October 9, 2007

ABSTRACT: 2,3-Benzodiazepine derivatives are drug candidates synthesized for potential treatment of various neurodegenerative diseases involving the excessive activity of AMPA receptors. Here we describe a rapid kinetic investigation of the mechanism of inhibition of the GluR2Q_{flip} AMPA receptor channel opening by two 2,3-benzodiazepine derivatives that are structurally similar (BDZ-2 and BDZ-3). Using a laser-pulse photolysis technique with a time resolution of ∼60 μs, we measured the effects of these inhibitors on both the channel opening rate and the whole-cell current amplitude. We found that both compounds preferably inhibit the open-channel state, although BDZ-2 is a more potent inhibitor in that it inhibits the open-channel state ∼5-fold stronger than BDZ-3 does. Both compounds bind to the same noncompetitive site. Binding of an inhibitor to the receptor involves the formation of a loose, partially conducting channel intermediate, which rapidly isomerizes to a tighter complex. The isomerization reaction is identified as the main step at which the receptor distinguishes the structural difference between the two compounds. These results suggest that addition of a bulky group at the N-3 position on the diazepine ring, as in BDZ-3, does not alter the mechanism of action, or the site of binding, but does lower the inhibitory potency, possibly due to an unfavorable interaction of a bulky group at the N-3 position with the receptor site. The new mechanistic revelation about the structure−reactivity relationship is useful in designing conformation-specific, more potent noncompetitive inhibitors for the GluR2 AMPA receptor.

Glutamate ion channels are classified into three subtypes: *N*-methyl-D-aspartic acid (NMDA), α-amino-3-hydroxy-5-methyl-4-isoxazolepropionic acid (AMPA),[1] and kainate receptors (*1*, *2*). AMPA receptors mediate the majority of fast excitatory neurotransmission in the mammalian central nerve system and are essential in brain activities such as memory and learning (*1*, *2*). Excessive activation of AMPA receptors is, however, known to induce calcium-mediated neurodegeneration, which underlies a variety of acute and chronic neurological disorders, such as post-ischemia cell death, Huntington's chorea, and amyotrophic lateral sclerosis (*2*). Developing AMPA receptor inhibitors to control the excessive receptor activity has been a long-pursued therapeutic approach to the treatment of these neurological disorders (*3*). To make new inhibitors more potent and selective for AMPA receptors, the mechanism of action of existing inhibitors needs to be investigated, and the structure−reactivity relationship for those structurally related compounds needs to be characterized.

2,3-Benzodiazepine derivatives, also known as GYKI compounds, represent one of the best classes of inhibitors in terms of their selectivity and affinity for AMPA receptors. GYKI 52466 [1-(4-aminophenyl)-4-methyl-7,8-methylenedioxy-5*H*-2,3-benzodiazepine] is the first inhibitor in this class discovered in the 1980s (*4*). Since then, hundreds of 2,3-benzodiazepine derivatives have been synthesized (*5*−*7*). GYKI compounds are considered allosteric regulators or noncompetitive inhibitors, a conclusion drawn largely from binding studies using radioactive agonists (*6*). However, the detailed mechanism by which 2,3-benzodiazepines inhibit AMPA receptors is not well documented. This deficiency can be mainly ascribed to the fact that an AMPA receptor opens its channel on the microsecond time scale following glutamate binding (*8*−*10*) but is desensitized or becomes inactivated while glutamate remains bound even on the millisecond time scale (*11*). As a result, the agonist binding assay is most relevant to characterization of the inhibitory effect on desensitized receptors. To assess the channel opening reaction for AMPA receptors, we have previously used a laser-pulse photolysis technique, together with a photolabile precursor of glutamate or the caged glutamate [i.e., γ-*O*-(α-carboxy-2-nitrobenzyl)glutamate] (*12*). We have shown that a channel opening reaction can be measured prior to the channel desensitization (*8*, *10*, *13*, *14*).

Here we investigated the mechanism of inhibition of the opening of the GluR2Q_{flip} channel by two 2,3-benzodiazepine compounds, 1-(4-aminophenyl)-3,5-dihydro-7,8-methylenedioxy-4*H*-2,3-benzodiazepin-4-one (BDZ-2) and its 3-*N*-

† This work was supported in part by grants from the Department of Defense (W81XWH-04-1-0106), the ALS Association, and the American Heart Association (0130513T) (to L.N.).

* To whom correspondence should be addressed. Telephone: (518) 591-8819. Fax: (518) 442-3462. E-mail: lniu@albany.edu.

‡ University at Albany, State University of New York.

§ Università di Messina.

[1] Abbreviations: AMPA, α-amino-3-hydroxy-5-methyl-4-isoxazolepropionic acid; BDZ, 2,3-benzodiazepine compounds; GYKI 52466, 1-(4-aminophenyl)-4-methyl-7,8-methylenedioxy-5*H*-2,3-benzodiazepine; caged glutamate, γ-*O*-(α-carboxy-2-nitrobenzyl)glutamate; HEK cells, human embryonic kidney cells.

10.1021/bi700782x CCC: $40.75
Published on Web 12/28/2007

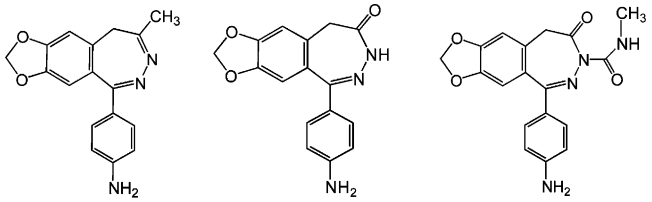

FIGURE 1: Chemical structures of GYKI 52466, BDZ-2, and BDZ-3. The chemical names for these compounds are given in the text.

methylcarbamoyl derivative (BDZ-3) (*15*) (Figure 1). BDZ-2 and BDZ-3 are structurally related to GYKI 52466, a template based on which many derivatives are synthesized (Figure 1). Compared to GYKI 52466, the 4-methyl group is replaced by a carbonyl group in both BDZ-2 and BDZ-3. The $GluR2Q_{flip}$ channel was chosen for this study because the GluR2 subunit in the unedited or Q (glutamine) isoform is known to control the calcium permeability of heteromeric AMPA receptors (*16*, *17*) and is thus considered a key subunit mediating excitotoxicity (*18*). The effect of an inhibitor on the channel opening and channel closing rate constants as well as the whole-cell current amplitude was determined with human embryonic kidney (HEK-293) cells that expressed the $GluR2Q_{flip}$ AMPA channels. Our results show that BDZ-2 and BDZ-3 bind to the same site, and both preferably inhibit the open-channel state of the $GluR2Q_{flip}$ receptor, although BDZ-2 is a stronger noncompetitive inhibitor. Furthermore, the inhibition of the receptor channel by these compounds likely involves the formation of a loose, partially conducting inhibitor−receptor intermediate, which rapidly isomerizes to a tighter, inhibitory complex. The implication of these results on the structure−reactivity relationship for developing more potent, conformation-specific 2,3-benzodiazepine derivatives is discussed.

EXPERIMENTAL PROCEDURES

Cell Culture and Receptor Expression. HEK-293S cells were cultured in Dulbecco's modified Eagle's medium supplemented with 10% fetal bovine serum and in a 37 °C, 5% CO_2, humidified incubator. $GluR2Q_{flip}$ was transiently expressed in these cells using a calcium phosphate method (*8*). HEK-293S cells were also cotransfected with a plasmid encoding green fluorescent protein and a separate plasmid encoding large T-antigen (*19*). The weight ratio of the plasmid for GluR2 to that for green fluorescent protein and large T-antigen was 1:0.2:10, and the $GluR2Q_{flip}$ plasmid used for transfection was ∼5−10 μg/35 mm dish. After 48 h, the transfected cells were used for recording.

Whole-Cell Current Recording. A recording electrode was made from a glass capillary (World Precision Instruments, Sarasota, FL) and had a resistance of ∼3 MΩ when filled with the electrode buffer. The electrode buffer was composed of 110 mM CsF, 30 mM CsCl, 4 mM NaCl, 0.5 mM $CaCl_2$, 5 mM EGTA, and 10 mM HEPES (pH 7.4, adjusted with CsOH). The external buffer contained 150 mM NaCl, 3 mM KCl, 1 mM $CaCl_2$, 1 mM $MgCl_2$, and 10 mM HEPES (pH 7.4, adjusted with NaOH). The whole-cell current was recorded with a cell voltage clamped at −60 mV, using an Axopatch-200B amplifier at cutoff frequency of 2−20 kHz by a built-in, eight-pole Bessel filter, and digitized at a sampling frequency of 5−50 kHz using an Axon Digidata 1322A instrument. The data were acquired using pCLAMP 8 (Molecular Devices, Sunnyvale, CA). All recordings were performed at room temperature. Unless otherwise noted, each data point was the average of at least three measurements collected from at least three cells.

Laser-Pulse Photolysis Measurements. The use of the laser-pulse photolysis technique to measure the channel opening kinetics has been described previously (*8*). Briefly, the caged glutamate (*12*) (Invitrogen, Carlsbad, CA) was dissolved in the external buffer and applied to a cell using a flow device (*20*) (see below). In the laser-pulse photolysis measurement of channel opening, a single laser pulse at 355 nm with a pulse length of 8 ns was generated from a pulsed Q-switched Nd:YAG laser (Continuum, Santa Clara, CA). The pulse energy varied in the range of 200−800 μJ, measured at the end of an optical fiber (300 μm core diameter) to which the laser beam was coupled. To calibrate the concentration of photolytically released glutamate, we applied two solutions of free glutamate with known concentrations to the same cell before and after a laser flash (*9*). The current amplitudes obtained from this calibration were compared with the amplitude from the laser measurement with reference to the dose−response relationship. These measurements also allowed us to monitor any damage to the receptors and/or the cell for successive laser experiments with the same cell (*8*).

To deliver an inhibitor to a cell, we used a "Ψ"-shaped flow device (*21*). The central tubing in the Ψ device was filled with an inhibitor solution for preincubation such that the solution was applied prior to the application of free glutamate as the control or free glutamate but mixed with the same inhibitor at the same concentration. In all experiments reported in this study, a 3 s preincubation flow protocol was required for both BDZ-2 and BDZ-3 to exert full inhibition of the receptor; a preincubation longer than 3 s caused no further current reduction. Furthermore, the 3 s preincuabtion for the ensuing inhibition was independent of glutamate concentration (and thus independent of the receptor form; see the explanation in the text). When the free glutamate was used to induce the receptor response in the absence and presence of an inhibitor, the amplitude of the whole-cell current observed using the flow device was corrected for receptor desensitization by a method previously described (*20*). The corrected current amplitude was used for data analysis.

Experimental Design and Data Analysis. To investigate the mechanism of inhibition, the effects of BDZ-2 or BDZ-3 on the channel opening rate constant (k_{op}) and channel closing rate constant (k_{cl}) were determined. These measurements were carried out at two glutamate concentrations by the following rationale. The observed rate constant (k_{obs}) of $GluR2Q_{flip}$ channel opening is a function of ligand concentration (see eq 2; eq 2 and all other equations are in the Appendix), which includes both rate terms, k_{op} and k_{cl}. This is particularly true experimentally when the molar concentration of ligand or glutamate (L) is either comparable to or larger than the value of the intrinsic equilibrium constant for the ligand (K_1) (*8*). However, when the ligand concentration is lowered (i.e., $L \ll K_1$), the k_{obs} expression or eq 2 is reduced to $k_{obs} \approx k_{cl}$. Under such a condition, the effect of an inhibitor on, and its inhibition constant for, the open-

channel state can be determined (eq 4). At a higher ligand concentration, where $k_{obs} > k_{cl}$, the k_{op} value can be determined from the difference between k_{obs} and k_{cl} or by rearranging eq 2 in that $k_{obs} - k_{cl} = k_{op}[L/(L + K_1)]^2$. Accordingly, the effect of the inhibitor on k_{op} and the inhibition constant for the closed-channel state can be measured (eq 5). Previously, we measured k_{op} and k_{cl} for $GluR2Q_{flip}$ (*8*) and also established the criteria under which k_{cl} can be determined from the measurement of k_{obs} (*8*, *9*). For $GluR2Q_{flip}$, k_{cl} is numerically equal to the k_{obs} obtained at ~100 μM glutamate, which corresponded to ~4% of the fraction of the open-channel form (*8*).

The experimental design of using current amplitude to determine the inhibition constant for both the open-channel and closed-channel states required varying concentrations of glutamate (see eqs 6a and 6b). Specifically, at low glutamate concentrations (i.e., $L \ll K_1$), the majority of the receptor was in the closed-channel state (see Figure 5; defined as the unliganded, singly liganded, and doubly liganded forms). Under this condition, the inhibition constant for the closed-channel state was determined from the ratio of the amplitude (see eqs 6a and 6b). Likewise, at a saturating ligand concentration (i.e., $L \gg K_1$), the majority of the receptor was in the open-channel state. Consequently, the inhibition constant associated with the open-channel state was measured. The basis of using the two ligand concentrations that corresponded to ~4 and ~95% of the open-channel form (*8*) to determine the corresponding inhibition constant was a putative difference in affinity with which a compound inhibited the receptor as a function of agonist concentration. At those very low and very high ligand concentrations (*8*), the apparent inhibition constants were considered pertinent to the closed-channel and open-channel states, respectively.

In double-inhibitor experiments where two inhibitors were used at the same time, the concentration of one inhibitor was kept constant while the concentration of the other was varied (eqs 7 and 8). In these experiments, only the amplitude in the presence (A_I) and absence (A) of two inhibitors was determined. All of the other conditions were the same as described before.

Origin 7 (Origin Lab, Northampton, MA) was used for both linear and nonlinear regressions (Levenberg−Marquardt and simplex algorithms). The error reported refers to the standard error of the fits, unless noted otherwise.

RESULTS

BDZ-2 and BDZ-3 are previously known to inhibit endogenous AMPA receptors in native tissues (*15*). Whether they specifically inhibit the GluR2 AMPA receptor subunit is unclear. Here, we first determined that BDZ-2 and BDZ-3 inhibited the $GluR2Q_{flip}$ receptor, as evidenced, for example, by the reduction of the amplitude of the glutamate-induced whole-cell current via the GluR2 channel in the presence of an inhibitor (Figure 2). At all concentrations of inhibitors and glutamate that were tested, neither inhibitor affected the rate of receptor desensitization, consistent with earlier reports for this class of inhibitors in general (*22*, *23*). We thus focused our investigation of the effect of an inhibitor on both the rate of the channel opening and the maximum current amplitude. For clarity, however, we present experimental data mostly for BDZ-2 since the BDZ-3 data are qualitatively the same.

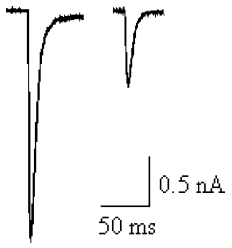

FIGURE 2: Representative whole-cell current traces via $GluR2Q_{flip}$ channels expressed in HEK-293 cells in the absence (left) and presence (right) of BDZ-2. The concentrations of glutamate and the inhibitor were 3 mM and 10 μM, respectively. The whole-cell current was recorded at −60 mV, pH 7.4, and 22 °C.

Effect of BDZ-2 and BDZ-3 on the Channel Opening Rate Constants. The rise of the whole-cell current via the $GluR2Q_{flip}$ channel, initiated by laser photolysis of the caged glutamate, reflected channel opening (Figure 3A) (*8*). As compared to the control, the current rise was slowed and the amplitude was concomitantly reduced in the presence of BDZ-2 (Figure 3A), consistent with the notion that BDZ-2 inhibited the channel opening of $GluR2Q_{flip}$. Furthermore, the observed rate constant in the absence (k_{obs}) and presence of BDZ-2 (k_{obs}') followed a first-order rate expression (eq 1) for ~95% of the rising phase (Figure 3A). Such a monophasic rate process was observed at both 100 ± 10 and 250 ± 20 μM photolytically released glutamate and at all concentrations of either inhibitor, consistent with the assumption that (a) the binding of glutamate and/or inhibitors to the receptor was fast relative to channel opening and (b) the decrease of the rate of channel opening in the presence of inhibitor was a result of receptor inhibition. Furthermore, the rate of desensitization, seen as a current decay (Figure 3A), at any given glutamate concentration in the absence (*8*−*10*, *14*) and presence of an inhibitor at any concentration was at least 10-fold slower than the rate of current rise, suggesting that the channel opening rate could be measured as a distinct kinetic process in the presence of an inhibitor. Thus, the observed rate constant of the channel opening, i.e., k_{obs} or k_{obs}', was calculated (using eq 1) without the complication of desensitization. As such, the mechanism of inhibition of the receptor channel opening (in Figure 5) was formulated without desensitization.

The effects of BDZ-2 on k_{op} and k_{cl} were determined (Figure 3B,C; see also Experimental Procedures for the experimental design). As seen here, BDZ-2 affected k_{cl} (Figure 3B) and k_{op} (Figure 3C). These results indicated that BDZ-2 inhibited both the closed-channel and open-channel states (the inhibition constants for both inhibitors are summarized in Table 1). Our findings are consistent with a noncompetitive inhibition by these compounds (*15*) and suggest that there are regulatory sites to which these inhibitors can bind and inhibit the channel. The effect of BDZ-2 and BDZ-3 on the current amplitude, described below, is also consistent with this conclusion (Table 1).

BDZ-2 and BDZ-3 Inhibited the Channel Opening by a Two-Step Process. We now examine the reduction of the whole-cell current amplitude in the presence of inhibitor. BDZ-2, for instance, reduced the amplitude of the whole-cell response and concurrently slowed the rate of channel opening (Figure 3A). An inhibition constant was calculated from the ratio of the maximum current amplitude in the absence and presence of BDZ-2 as a function of its

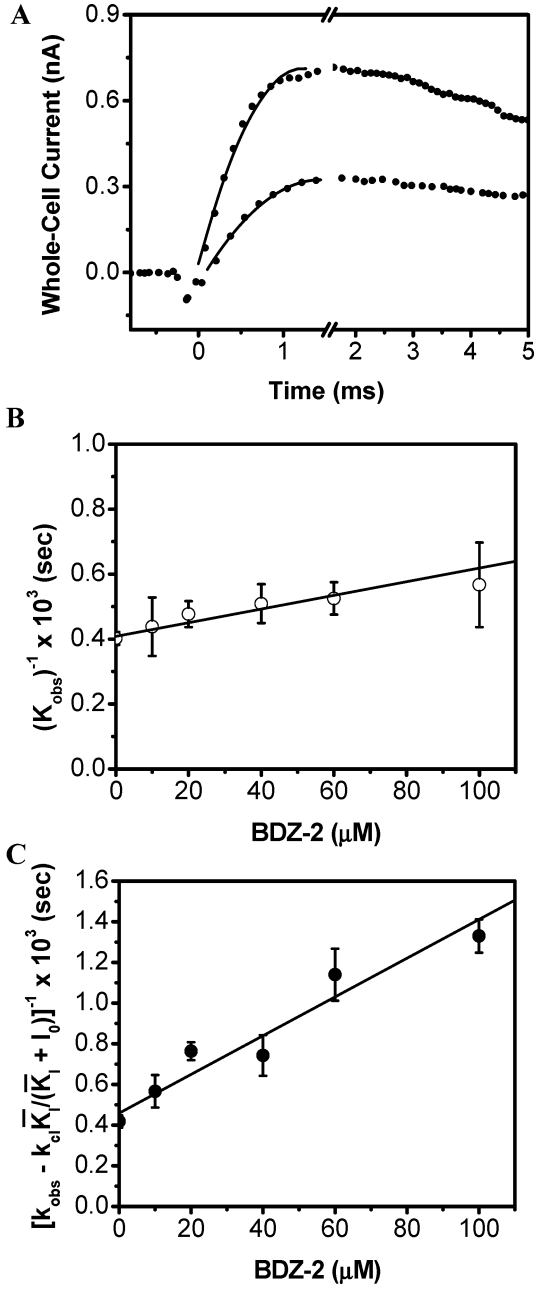

FIGURE 3: Effect of BDZ-2 on the channel opening rate constants. (A) Representative whole-cell current traces from the laser-pulse photolysis experiment showing that BDZ-2 inhibited both the rate and the amplitude of the opening of the GluR2Q_{flip} channel. The top trace is the control (k_{obs} = 2519 s^{-1}; A = 0.70 nA), and the bottom one included 20 μM BDZ-2 (k_{obs} = 2114 s^{-1}; A_I = 0.33 nA). In both traces, the concentration of the photolytically released glutamate was estimated to be 150 μM. (B) Effect of BDZ-2 on k_{cl} obtained at 100 μM glutamate and as a function of BDZ-2 concentration. From this plot, a $\overline{K_I}$* of 194 ± 20 μM was obtained, using eq 4. (C) Effect of BDZ-2 on k_{op} obtained at 250 μM glutamate and as a function of BDZ-2 concentration. From this plot, a K_I^* of 48 ± 5 μM was determined, using eq 5. All of the inhibition constants are summarized in Table 1.

concentration (eq 6 and Figure 4). However, the inhibition constant for both the open-channel and closed-channel states, obtained from the amplitude measurement, was always found to be smaller than the corresponding value obtained from the rate measurement (Table 1). A one-step inhibition model in which the binding of an inhibitor to the receptor directly led to a complete inhibition could not account for this

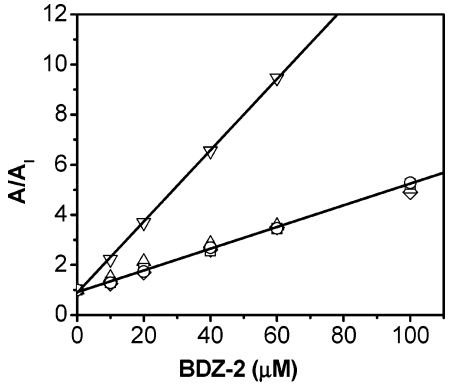

FIGURE 4: Effect of BDZ-2 on the amplitude of the whole-cell current in the absence (A) and presence (A_I) of BDZ-2. An inhibition constant was calculated from this plot using eq 6. At 3 mM glutamate (▽), a $\overline{K_I}$ of 6.9 ± 1.0 μM was obtained, corresponding to the inhibition constant for the open state; a K_I of 24.8 ± 1.0 μM was obtained for the closed-channel state at a glutamate concentration of 100 μM (◇). In both cases, the amplitude was from the flow measurements. From laser-photolysis measurements, a K_I of 25.2 ± 1.0 μM was obtained from the data at 100 μM glutamate and varied concentrations of BDZ-2 (△). At 250 μM glutamate (○), the $\overline{K_I}$ was determined to be 23.0 ± 1.0 μM.

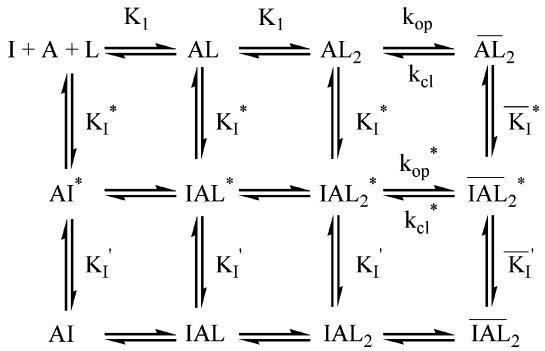

FIGURE 5: Minimal mechanism of the inhibition of the GluR2Q_{flip} receptor by BDZ-2 and BDZ-3 involving an intermediate state. L represents ligand or glutamate, and the number of ligands that bind to and open the channel is assumed to be two (*8*). Here, A represents the active, unliganded form of the receptor, and I represents an inhibitor. For simplicity and without contrary evidence, it is assumed that glutamate binds with equal affinity or K_1, the intrinsic equilibrium dissociation constant, at all binding steps. All the species with an asterisk symbolize those at the intermediate state, whereas those species bound with inhibitor but without an asterisk represent those of the final state. All species related to A, AL, and AL_2, including those bound with inhibitors, are in the closed-channel state, whereas those related to $\overline{AL_2}$ refer to the open-channel state.

discrepancy (*24*). With such a model, the inhibition constant obtained from the rate measurement would be the same as the one obtained from the current amplitude (*24*). However, the discrepancy could be ascribed to a minimal mechanism (in Figure 5) in which the binding of BDZ-2 or BDZ-3 to the receptor initially formed an intermediate (e.g., $\overline{IAL_2}$*) in the first step, and such an intermediate was partially conducting; in the second step, the intermediate isomerized rapidly to form an inhibitory complex ($\overline{IAL_2}$). The two-step inhibition process would apply to both the closed-channel and open-channel states, on the basis of our experimental results (Figure 3B,C).

Using this isomerization model (Figure 5), the discrepancy in the magnitude of the inhibition constant between the rate and the amplitude measurements can now be explained. First,

Table 1: Inhibition Constants of BDZ-2 and BDZ-3, Obtained from Rate and Amplitude Measurements, for the Closed-Channel and Open-Channel States of GluR2Q$_{flip}$

	rate measurement[a]			amplitude measurement		
	K_I^* (μM)[b] (closed channel)	$\overline{K_I}$* (μM)[b] (open channel)	K_I (μM)[b,d]	$\overline{K_I}$ (μM)[b,e]	K_I (μM)[c,d] (closed channel)	$\overline{K_I}$ (μM)[c,f] (open channel)
BDZ-2	48 ± 5	194 ± 20	25.2 ± 1.0	23.0 ± 1.0	24.8 ± 1.0	6.9 ± 1.0
BDZ-3	514 ± 60	204 ± 18	200 ± 18	69 ± 4.0	210 ± 20	38 ± 10

[a] The constants obtained from rate measurements represent those in the first step of inhibition as in Figure 5, whereas those obtained from the amplitude measurements represent the overall inhibition constants. [b] Laser-pulse photolysis measurement. [c] Cell-flow measurement. [d] Measurements at 100 μM glutamate for the closed-channel state. [e] Measurements at 250−350 μM glutamate. [f] Measurements at 3 mM glutamate.

the maximum current amplitude was related to the fraction of the open-channel form at the quasi-equilibrium level, which depended on glutamate concentration (see eq 6b). Therefore, a smaller inhibition constant or a stronger inhibition obtained from the amplitude measurement, as compared with the corresponding inhibition constant from the rate measurement at the same glutamate concentration, suggested that the magnitude of the receptor inhibition obtained from the rate measurement could not account for the total inhibition. An additional step, followed by the formation of the initial, partially conducting receptor−inhibitor intermediate, must be involved to presumably turn the intermediate into a tighter complex, thereby yielding additional inhibition. This assumption is supported by a ratio of inhibition constants being ~28 for the open-channel state (i.e., 194 μM/6.9 μM) in the case of BDZ-2 and a ratio of ~2 for the closed-channel state (i.e., 48 μM/24.8 μM) (in Table 1). BDZ-3 showed a similar, albeit less significant, reduction of the corresponding inhibition constant via the second step (Table 1). Second, a single-exponential current rise for the opening of the channel (Figure 3B) was always observed at all concentrations of the inhibitor (and glutamate), suggesting that the rate constants associated with the two steps in the presence of an inhibitor (Figure 5) were significantly different. If the two rates in the presence of an inhibitor were comparable, a double-exponential rate process would be expected at a certain concentration range of an inhibitor during the whole-cell current rise. Furthermore, the $1/k_{obs}'$ increased linearly with an increase in inhibitor concentration, as predicted by eqs 3−5 derived from one-step inhibition (i.e., the scheme only involving the top and middle rows in Figure 5 with the assumption that the second step is much faster than the first step). Such a linear correlation remained at different glutamate concentrations where the effects of an inhibitor on both k_{cl} and k_{op} were determined (Figure 3B,C). As a result, this linearity allowed us to calculate $\overline{K_I}$* and K* for the intermediate associated with the open channel and closed channel, respectively. If the second step were slow and were measured during the rising phase of the whole-cell current, then the one-step inhibition model should have fully accounted for the inhibition. Consequently, the inhibition constant obtained from the rate measurement would have been identical to the corresponding value obtained from the amplitude measurement (*24*).

Effect of BDZ-2 and BDZ-3 on the Whole-Cell Current Amplitude Determined in Flow Measurements. As an independent approach to evaluation of inhibition constants for both BDZ-2 and BDZ-3 based on the whole-cell current amplitude, we also used a solution flow technique with known concentrations of free glutamate and measured the whole-cell current amplitude in the absence and presence of an inhibitor. The experimental design of using current amplitude to determine the inhibition constants for both the open-channel and closed-channel states required varying concentrations of glutamate (see Experimental Procedures and eqs 6a and 6b). Here, glutamate concentrations from 100 μM to 5 mM were chosen, which corresponded to the fraction of the open-channel form being from ~4 to ~95%, respectively [note that the channel opening probability for this receptor is 96% (*8*)]. The apparent inhibition constants for both BDZ-2 and BDZ-3 were therefore determined at these glutamate concentrations (Figure 4 and Table 1).

Several conclusions can be drawn from these results. First, at a comparable glutamate concentration such as 100 or 250 μM, the A/A_I ratios determined from the flow measurements were identical, within experimental error, to those obtained from the laser-pulse photolysis measurements for both inhibitors (Table 1). Second, at 3 mM glutamate where ~93% of the channels were in the open-channel state, the apparent inhibition constant was considered virtually a measure of the affinity of BDZ-2 for the open-channel state, $\overline{K_I}$, of the GluR2Q$_{flip}$ receptor (see eq 6). Thus, comparison of $\overline{K_I}$ with K_I, the inhibition constant for the closed-channel state, shows that BDZ-2 inhibits the open-channel state ~3.6-fold more strongly (Table 1). BDZ-3, on the other hand, shows a 5-fold stronger inhibition for the open-channel state (Table 1). Third, BDZ-2 is a more potent inhibitor, because it has 5.5- and 8-fold higher affinities for the open-channel and closed-channel states of GluR2Q$_{flip}$, respectively, than BDZ-3 does.

BDZ-2 and BDZ-3 Bind to the Same Inhibitory Site on the GluR2Q$_{flip}$ Receptor. On kinetic grounds (Table 1), BDZ-2 and BDZ-3 share essential functional similarities in that each inhibitor binds to a regulatory (i.e., inhibitory) site on the GluR2Q$_{flip}$ receptor; both inhibit preferentially the open-channel state, although BDZ-2 is a stronger noncompetitive inhibitor. Given the structural similarity between these two compounds (Figure 1), we asked whether they competed for the same regulatory site or bound to two different sites on the receptor. The answer to this question shall have a meaningful implication in improving our understanding of the structure−reactivity relationship of the GYKI compound series, particularly in the prediction of the putative consequence of derivatization at the N-3 position of the diazepine ring.

To address whether the two compounds competed for one inhibitory site or bound separately to two sites, we carried out a double-inhibitor experiment (see Experimental Proce-

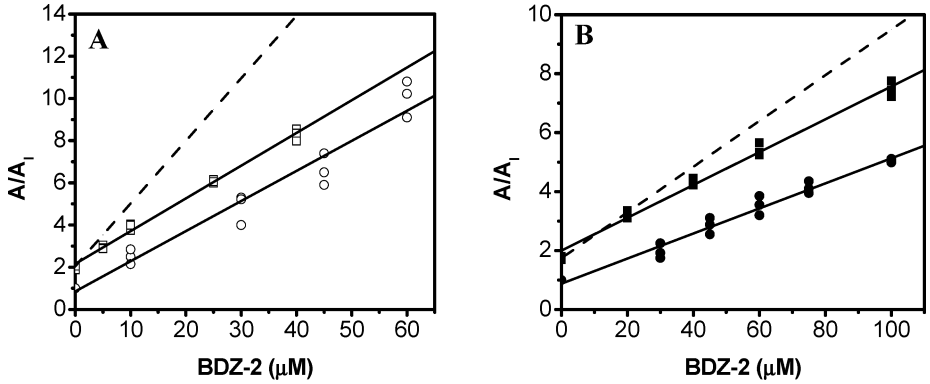

FIGURE 6: Double-inhibition experiments involving both BDZ-2 and BDZ-3. (A) Double inhibition of the open-channel state (3 mM glutamate) of the GluR2Q$_{flip}$ receptor by both BDZ-2 and BDZ-3. The concentration of BDZ-3 was fixed at 40 μM, whereas the concentration of BDZ-2 was varied. The empty circles represent data for BDZ-2 only, and the empty squares represent data for double inhibition by both BDZ-2 and BDZ-3. The K_I of the double inhibition is 6.4 $\pm$ 0.2 μM compared to the value of 6.9 $\pm$ 0.5 μM for just BDZ-2 (Table 1). (B) Double inhibition of the closed-channel state (100 μM glutamate) of the GluR2Q$_{flip}$ receptor by both BDZ-2 and BDZ-3. The concentration of BDZ-3 was fixed at 100 μM, whereas that of BDZ-2 was varied. The filled circles represent data for BDZ-2 only, while the filled squares represent data for both BDZ-2 and BDZ-3. The K_I of the double inhibition was found to be 19.0 $\pm$ 1.0 μM, compared to the K_I of 22.0 $\pm$ 2.0 μM for just BDZ-2 (Table 1). Note that all of the amplitudes used here were from solution-flow measurements. In both panels A and B, the top solid line represents the best fit to the data of the double-inhibition experiments, using eq 7, the one-site model (in the Appendix), compared to the bottom solid line which is the best fit to the data of the single-inhibitor experiment, using eq 6. The dashed line in both panels A and B is the simulated double-inhibition result from eq 8, assuming that the two inhibitors bind to two different sites.

dures and Appendix). The comparison of the ratio of the current amplitude in the absence and presence of two inhibitors with the ratio in the presence of just one inhibitor showed that the slope from which a $K_{I,app}$ value was determined (using eq 7) remained invariant even when the second inhibitor was additionally present (Figure 6). This result suggested that BDZ-2 and BDZ-3 bound to the same site (alternatively, they could bind to two sites, but the binding of the two sites would be mutually exclusive). This conclusion was mutually affirmed from the experiments at two different concentrations of glutamate (Figure 6), which correlated to the open-channel and closed-channel states. Conversely, if BDZ-2 and BDZ-3 bound to two different sites independently, the inhibition would be "additive" or stronger than that of either inhibitor alone, due to an effective increase in the overall concentration of inhibitors bound to the two sites (the dashed line in Figure 6A,B).

DISCUSSION

In this study, we investigated the mechanism of inhibition and the site of interaction for two structurally related inhibitors, BDZ-2 and BDZ-3 (Figure 1). Using the laser-pulse photolysis technique, which previously enabled us to characterize the channel opening rate process of GluR2Q$_{flip}$ (*8*), we measured the effect of each inhibitor on k_{op} and k_{cl} as well as the whole-cell current amplitude. Our findings reveal new features for the mechanism of action and the structure−reactivity relationship of these compounds.

Site of Interaction of BDZ-2 and BDZ-3 with the GluR2Q$_{flip}$ Receptor and Structure−Reactivity Relationship. Both BDZ-2 and BDZ-3 were found to inhibit the GluR2Q$_{flip}$ channel noncompetitively. This conclusion was based on the finding that each of these compounds affected k_{op} and k_{cl}. If BDZ-2, for instance, inhibited the channel uncompetitively, commonly known as open-channel blockade, only the effect on k_{cl}, not that on k_{op}, would be expected; i.e., the $k_{obs} - k_{cl}'$ term in eq 5 would be independent of inhibitor concentration. On the other hand, if BDZ-2 inhibited the channel competitively, only the effect on k_{op}, not that on k_{cl}, would be expected. Furthermore, it is equally important to note that, as observed in both the photolysis and flow measurements, BDZ-2 also inhibited the whole-cell current under the conditions where the open-channel and closed-channel states were measured. Therefore, the effects of BDZ-2 on both the rate constants and the current amplitude are all consistent with the conclusion that BDZ-2 is a noncompetitive inhibitor. The same conclusion can be drawn for BDZ-3.

BDZ-2 and BDZ-3 were also found to compete for the same noncompetitive site on GluR2Q$_{flip}$. Both inhibitors exhibit a higher affinity for the open-channel state of the receptor, although BDZ-2 is a stronger inhibitor. It seems that derivatizing BDZ-2 by addition of a methylcarbamoyl group at the N-3 position of the benzodiazepine ring, resulting in BDZ-3, preserves the same mechanism of action but decreases the overall potency for BDZ-3. One plausible explanation is that the same binding site on the receptor does not prefer to accommodate a bulky group at the N-3 position. We therefore hypothesize that addition of a bulky group at the N-3 position, based on the BDZ-2 template, will yield a compound that prefers to inhibit the open-channel conformation of GluR2Q$_{flip}$ but with a weakened potency.

However, several issues remain. First, the kinetic evidence that enabled us to deduce the site of interaction for BDZ-2 and BDZ-3 with the receptor does not provide the clue for the location of this site (except it is distinct from the agonist binding site). In an attempt to address this question, we performed preliminary NMR experiments using ^{15}N-labeled S1S2 derived from the GluR2Q$_{flip}$ receptor but found no change in chemical shifts when BDZ-2 was mixed with S1S2 (Jayaseelan, Shekhtman, and Niu, unpublished result). One possibility is that the S1S2 protein does not contain the noncompetitive site to which BDZ-2 binds (as a control, mixing of either glutamate or NBQX, a competitive antagonist, with S1S2 did show changes in chemical shifts). A previous study by Balannik et al. (*25*) with a different GYKI compound (i.e., GYKI 53655) suggested that the site of interaction is near the interface between the extracellular binding domain of S1S2 of an AMPA receptor and lipid

bilayer. Balannik and co-workers (*25*) also identified specific amino acid residues affecting the receptor sensitivity to this compound, which are part of the sequences linking the C-termini of S1 and S2 to the transmembrane segments of M1 and M4 or the S1−M1 and S2−M4 regions. However, the linker sequences which cover these residues are not part of the S1S2 construct (*25*). It should be further noted that the C-terminus of S1S2 ends in the middle of the flip-flop region as compared to the full-length receptor (*26*). Taken together, the S1S2 construct is likely incomplete in forming the site for noncompetitive inhibitors, as previously suggested (*25*).

Second, it is not yet known what the structural feature(s) confers the open-channel preferring property to both compounds. What these compounds have in common, as compared with the structure of the parent compound, GYKI 52466 (Figure 1), is the fact that the methyl group at position 4 in the benzodiazepine ring of GYKI 52466 is replaced by a carbonyl group in both BDZ-2 and BDZ-3. Whether this replacement makes a difference in conferring such a preference awaits further study of additional inhibitors, such as GYKI 52466.

Mechanism of Action for BDZ-2 and BDZ-3. Both BDZ-2 and BDZ-3 appear to operate in a two-step process to inhibit the receptor channel. In the first step, an inhibitor forms a loose complex with the receptor, resulting in a partially inhibited channel. In the second step, the intermediate rapidly isomerizes to a tighter complex. This two-step process is evident in a comparison of the inhibition constants associated with the first step and the overall reaction (Table 1). For instance, the inhibition constant for the first step or $\overline{K_I}^*$ is 194 μM for BDZ-2, whereas the overall inhibition constant, $\overline{K_I}$, becomes ~7 μM, reflecting a 28-fold higher potency after an isomerization reaction. This comparison suggests that the initial step, resulting in the formation of an inhibitor−receptor intermediate, is far from sufficient to account for the full inhibition.

However, the incomplete inhibition through the initial inhibitor−receptor channel is unlikely a result of inadequate equilibration of an inhibitor with the receptor site, although a 3 s preincubation was required for a full inhibition. Such a preincubation time would be too long to be considered relevant to a bimolecular rate process for the binding of these compounds to the receptor site in this case. In one scenario that can explain a long preincubation phenomenon for an inhibitor with a fast binding reaction, a slow diffusional access of an inhibitor to its site is required because the site is covered by membrane or is a buried one. Given the results from Balannik et al. (*25*) and our results from a NMR study of the S1S2 binding domain, it is possible that the site to which BDZ-2 and BDZ-3 bind is a buried one. However, in spite of slow diffusional access, subsequent steps can be very fast (but the inhibition can be measured only when the bound activating ligand initiates the channel opening process). On the other hand, if there were a slow inhibitor binding reaction so that the binding could not be treated as a rapid equilibrium on the time scale of channel opening, several phenomena would be anticipated. First, on the time scale of channel opening, we would have measured a bimolecular association reaction, rather than an inhibition reaction. As a result, the observed rate at a fixed glutamate concentration would have been higher as the concentration of inhibitor had increased. However, we observed just the opposite (i.e., k_{obs} was slower when the inhibitor concentration increased). Second, could the binding reaction be so slow that the inhibition occurred on one of the two time scales, both of which were after the channel opening: the inhibition occurred (a) in parallel to the time course for desensitization or (b) after the channel had desensitized or in a second time scale? In both cases, the current amplitude would appear to be smaller or "inhibited" because we would have measured the portion of the receptors without any inhibitors bound. However, neither the desensitization rate nor the rate of channel activity recovery (after the channel was pre-exposed to inhibitor and glutamate) was affected (data not shown); these are the same phenomena reported by Balannik et al. (*25*) for other GYKI compounds. We therefore conclude that the inhibition occurs on the time scale of channel opening, after a full equilibration, consistent with the assumption that the decrease in the rate of channel opening in the presence of an inhibitor was due to inhibition.

Classical examples of a two-step inhibition involving enzyme inhibitors are well documented (*27*, *28*). Mechanisms similar to the one proposed in this study (Figure 5), involving a two-step inhibition process, have also been documented with the muscle nicotinic acetylcholine receptor with several inhibitors (*29*, *30*). For the inhibition of the nicotinic acetylcholine receptor by either cocaine (*29*) or MK-801 (*30*), the first step yields a corresponding channel that is thought to conduct cations as well as or even better than the channel without an inhibitor, thus exhibiting no inhibition on k_{obs} at either a low or a high ligand concentration. In the case of MK-801, the second step, which yields the nonconducting inhibitor−receptor complex, is thought to only occur through the open-channel state (*30*). In the case of BDZ-2 and BDZ-3, a two-step process occurs through both the closed-channel and open-channel states, which is evidenced by the decrease in k_{obs} at both low and high glutamate concentrations.

Implication of Receptor Properties and Structure−Reactivity Relationship. The results of this study (Table 1) reveal new features related to receptor properties and the structure−reactivity relationship for these compounds. The comparison of the overall inhibition constant between BDZ-2 and BDZ-3 shows that BDZ-2 inhibits the open-channel state >5-fold more strongly (see Table 1). However, the inhibition constant for the initial receptor−inhibitor complex for the open-channel state between the two inhibitors is identical [i.e., $\overline{K_I}^*$ is 194 ± 20 μM for BDZ-2 as compared to 204 ± 18 μM for BDZ-3 (Table 1)]. On the other hand, for the closed-channel state, the K_I^* value associated with the initial step for BDZ-2 is already 10-fold different from the value for BDZ-3 (i.e., 48 μM for BDZ-2 vs 514 μM for BDZ-3). Furthermore, when the overall inhibition for the closed-channel state is compared, the difference between BDZ-2 and BDZ-3 is now 8-fold (i.e., 24.8 μM for BDZ-2 vs 210 μM for BDZ-3). This comparison suggests that the isomerization reaction for the *closed-channel state* has merely resulted in ~2-fold improvement for "tightening" the complex for both inhibitors ($\overline{K_I}^*/\overline{K_I}$ = 48/24.8 for BDZ-2 and 514/210 for BDZ-3). In contrast, the receptor−inhibitor complex in the *open-channel state* must undergo an ~5-fold change for BDZ-3 [$\overline{K_I}^*/\overline{K_I}$ = 204/38 (see Table 1)] and

a staggering ~28-fold change for BDZ-2 (i.e., $\overline{K_I}^*/\overline{K_I}$ = 194/6.9). These results thus suggest that the closed-channel state bound with an inhibitor requires less conformational change to become a "tighter" complex than the open-channel state. One possible explanation is that the closed-channel forms are more "accommodating" to binding of inhibitors with different structures and are thus more "modifiable", at least in the first step, than the open-channel form. Our results further suggest that the first step associated with the open-channel state is not the one to distinguish the structural difference between BDZ-2 and BDZ-3, although both compounds preferentially inhibit the open-channel state. Rather, it is the putative isomerization reaction involving the open-channel state that "sees" or discriminates the bulkier side chain at the N-3 position for BDZ-3, resulting in the overall difference in the inhibitory properties between the two compounds. Our results are further consistent with the notion by which, as compared with the initial intermediate, the isomerized receptor−inhibitor complex is tighter, thus making it possible for a closer interaction between the binding site and a binder so that the structural difference between the two inhibitors is distinguished.

Using the rapid kinetic techniques, we show that the mechanism of action and the structure−reactivity relationship of the two 2,3-benzodiazepine derivatives can now be characterized in a more detailed fashion than previously possible. The new findings provide useful clues for the future design and synthesis of 2,3-benzodiazepine inhibitors that are more potent and more specific toward a unique receptor conformation. Our finding that BDZ-3 acts mechanistically the same as BDZ-2 and binds to the same site as BDZ-2 does, but is a weaker inhibitor, indicates that addition of a substituent to the N-3 position on the diazepine ring of BDZ-2, resulting in an increase in size at this position, is expected to generate a weaker inhibitor. However, our finding also suggests a possibility that a photolabel, for instance, can be attached to the N-3 position, and the resulting compound can serve as a site-directed reagent for labeling and mapping of the inhibitory site on the receptor. The location of the site, inferred from this study, is unknown. The location of this and any other regulatory site on any AMPA receptor subunit is in turn beneficial to the design and synthesis of newer 2,3-benzodiazepine derivatives.

APPENDIX

The channel opening rate process of GluR2Q_{flip}, initiated by a laser-pulse photolysis measurement with the caged glutamate, followed a single-exponential rate expression for ~95% of the rise time (*8*). This observation was without exception for all current traces induced by glutamate in the presence and absence of an inhibitor and was therefore consistent with the assumption that the binding of glutamate and/or inhibitor was fast relative to channel opening (*8*). An observed rate constant, k_{obs}, can be calculated from eq 1. In eq 1, I_t represents the current amplitude at time t and I_{max} the maximum current amplitude. Furthermore, using only the upper scheme in Figure 5 or the scheme without any inhibitor bound, k_{obs} can be formulated as in eq 2 to represent the channel opening reaction.

$$I_t = I_{max}(1 - e^{-k_{obs}t}) \quad (1)$$

$$k_{obs} = k_{cl} + k_{op}\left(\frac{L}{L + K_1}\right)^2 \quad (2)$$

When the channel opening rate was inhibited noncompetitively (as in Figure 5), the expression for the observed first-order rate constant was given by eq 3. The derivation of eq 3 was based on the assumption that only the first step was observable (i.e., this step was assigned to the reaction involving the formation of the initial inhibitor−receptor complex) and the second step (i.e., the step leading to the formation of the final receptor−inhibitor complex via a presumed isomerization reaction) was faster than the first step and faster than the rate of channel opening. As such, the effect of an inhibitor on k_{cl} was determined using eq 4, where the inhibition constant associated with the open-channel state ($\overline{K_I}^*$) could be determined (at a low ligand concentration; see the text for further explanation). At higher ligand concentrations, the effect of an inhibitor on k_{op} was determined from the difference between k_{obs} and k_{cl}', as shown in eq 5, and K_I^* was determined (*24*).

$$k_{obs} = k_{cl}\left(\frac{\bar{K}_I^*}{\bar{K}_I^* + I}\right) + k_{op}\left(\frac{L}{L + K_1}\right)^2\left(\frac{K_I^*}{K_I^* + I}\right) \quad (3)$$

$$\frac{1}{k_{obs}} = \frac{1}{k_{cl}} + \frac{1}{k_{cl}}\frac{I}{\bar{K}_I^*} \quad (4)$$

$$(k_{obs} - k_{cl}')^{-1} = [k_{op}L/(L + K_1)^2]^{-1}(1 + I/K_I^*) \quad (5)$$

An inhibition constant was also independently estimated from the ratio of the maximum current amplitudes in the absence, A, and presence, A_I, of an inhibitor, given by eq 6a.

$$\frac{A}{A_I} = 1 + I\frac{(\overline{AL_2})_O}{K_I} \quad (6a)$$

where $(\overline{AL_2})_O$ represents the fraction of the open-channel form and is proportional to the current amplitude. In eq 6b, this fraction is expressed as a function of the fraction of all receptor forms.

$$(\overline{AL_2})_O = \frac{\overline{AL_2}}{A + AL + AL_2 + \overline{AL_2}} = \frac{L^2}{L^2(1 + \Phi) + 2K_1L\Phi + K_1^2\Phi} \quad (6b)$$

Equation 6 permitted the calculation of the apparent overall inhibition constant at a defined agonist concentration. This is especially important for an inhibitor which exhibits a different affinity toward the open-channel and closed-channel states. In that case, the apparent inhibition constant, $K_{I,app}$, is further dependent on the agonist concentration.

To determine whether BDZ-2 and BDZ-3 bound to the same site or two different sites, the two inhibitors were used simultaneously to inhibit the channel activity (*31*). Specifically, the amplitude was measured and used, as in eq 6, to plot $A/A_{I,P}$ versus one inhibitor concentration (see Figure 6). Here, one inhibitor was represented as I while the other was P, all at molar concentrations. Assuming that one inhibitor

bound per receptor and binding of one inhibitor excluded the binding of the other (i.e., one-site model or AI or AP was allowed but not API), the ratio of the current amplitude was given by eq 7 (*31*).

$$\frac{A}{A_{I,P}} = \left(1 + \frac{P}{K_P}\right) + \frac{I}{K_I} \quad (7)$$

On the other hand, for a two-site model in which there were two sites for I and P, respectively (i.e., both AI and AP and API were all allowed), the ratio of the current amplitude was given by eq 8.

$$\frac{A}{A_{I,P}} = \left(1 + \frac{P}{K_P}\right) + \left(1 + \frac{P}{K_P}\right)\frac{I}{K_I} \quad (8)$$

ACKNOWLEDGMENT

We thank Gang Li in the lab for collecting some data on BDZ-3 and Christof Grewer for critical reading of the manuscript.

REFERENCES

1. Hollmann, M., and Heinemann, S. (1994) Cloned glutamate receptors, *Annu. Rev. Neurosci. 17*, 31−108.
2. Dingledine, R., Borges, K., Bowie, D., and Traynelis, S. F. (1999) The glutamate receptor ion channels, *Pharmacol. Rev. 51*, 7−61.
3. Brauner-Osborne, H., Egebjerg, J., Nielsen, E. O., Madsen, U., and Krogsgaard-Larsen, P. (2000) Ligands for glutamate receptors: Design and therapeutic prospects, *J. Med. Chem. 43*, 2609−2645.
4. Tarnawa, I., Farkas, S., Berzsenyi, P., Pataki, A., and Andrasi, F. (1989) Electrophysiological studies with a 2,3-benzodiazepine muscle relaxant: GYKI 52466, *Eur. J. Pharmacol. 167*, 193−199.
5. Zappala, M., Grasso, S., Micale, N., Polimeni, S., and De Micheli, C. (2001) Synthesis and structure-activity relationships of 2,3-benzodiazepines as AMPA receptor antagonists, *Mini-Rev. Med. Chem. 1*, 243−253.
6. Solyom, S., and Tarnawa, I. (2002) Non-competitive AMPA antagonists of 2,3-benzodiazepine type, *Curr. Pharm. Des. 8*, 913−939.
7. Zappala, M., Pellicano, A., Micale, N., Menniti, F. S., Ferreri, G., De Sarro, G., Grasso, S., and De Micheli, C. (2006) New 7,8-ethylenedioxy-2,3-benzodiazepines as noncompetitive AMPA receptor antagonists, *Bioorg. Med. Chem. Lett. 16*, 167−170.
8. Li, G., Pei, W., and Niu, L. (2003) Channel-opening kinetics of GluR2Q_{flip} AMPA receptor: A laser-pulse photolysis study, *Biochemistry 42*, 12358−12366.
9. Li, G., and Niu, L. (2004) How fast does the GluR1Qflip channel open? *J. Biol. Chem. 279*, 3990−3997.
10. Li, G., Sheng, Z., Huang, Z., and Niu, L. (2005) Kinetic mechanism of channel opening of the GluRDflip AMPA receptor, *Biochemistry 44*, 5835−5841.
11. Trussell, L. O., and Fischbach, G. D. (1989) Glutamate receptor desensitization and its role in synaptic transmission, *Neuron 3*, 209−218.
12. Wieboldt, R., Gee, K. R., Niu, L., Ramesh, D., Carpenter, B. K., and Hess, G. P. (1994) Photolabile precursors of glutamate: Synthesis, photochemical properties, and activation of glutamate receptors on a microsecond time scale, *Proc. Natl. Acad. Sci. U.S.A. 91*, 8752−8756.
13. Li, G., Oswald, R. E., and Niu, L. (2003) Channel-opening kinetics of GluR6 kainate receptor, *Biochemistry 42*, 12367−12375.
14. Pei, W., Huang, Z., and Niu, L. (2007) GluR3 flip and flop: Differences in channel opening kinetics, *Biochemistry 46*, 2027−2036.
15. Grasso, S., Micale, N., Zappala, M., Galli, A., Costagli, C., Menniti, F. S., and De Micheli, C. (2003) Characterization of the mechanism of anticonvulsant activity for a selected set of putative AMPA receptor antagonists, *Bioorg. Med. Chem. Lett. 13*, 443−446.
16. Jonas, P., and Spruston, N. (1994) Mechanisms shaping glutamate-mediated excitatory postsynaptic currents in the CNS, *Curr. Opin. Neurobiol. 4*, 366−372.
17. Geiger, J. R., Melcher, T., Koh, D. S., Sakmann, B., Seeburg, P. H., Jonas, P., and Monyer, H. (1995) Relative abundance of subunit mRNAs determines gating and Ca^{2+} permeability of AMPA receptors in principal neurons and interneurons in rat CNS, *Neuron 15*, 193−204.
18. Kwak, S., and Weiss, J. H. (2006) Calcium-permeable AMPA channels in neurodegenerative disease and ischemia, *Curr. Opin. Neurobiol. 16*, 281−287.
19. Huang, Z., Li, G., Pei, W., Sosa, L. A., and Niu, L. (2005) Enhancing protein expression in single HEK 293 cells, *J. Neurosci. Methods 142*, 159−166.
20. Udgaonkar, J. B., and Hess, G. P. (1987) Chemical kinetic measurements of a mammalian acetylcholine receptor by a fast-reaction technique, *Proc. Natl. Acad. Sci. U.S.A. 84*, 8758−8762.
21. Niu, L., Grewer, C., and Hess, G. P. (1996) *Chemical kinetic investigations of neurotransmitter receptors on a cell surface in a microsecond time region*, Vol. VII, Acadamic Press, New York.
22. Donevan, S. D., and Rogawski, M. A. (1993) GYKI 52466, a 2,3-benzodiazepine, is a highly selective, noncompetitive antagonist of AMPA/kainate receptor responses, *Neuron 10*, 51−59.
23. Rammes, G., Swandulla, D., Spielmanns, P., and Parsons, C. G. (1998) Interactions of GYKI 52466 and NBQX with cyclothiazide at AMPA receptors: Experiments with outside-out patches and EPSCs in hippocampal neurones, *Neuropharmacology 37*, 1299−1320.
24. Niu, L., and Hess, G. P. (1993) An acetylcholine receptor regulatory site in BC3H1 cells: Characterized by laser-pulse photolysis in the microsecond-to-millisecond time region, *Biochemistry 32*, 3831−3835.
25. Balannik, V., Menniti, F. S., Paternain, A. V., Lerma, J., and Stern-Bach, Y. (2005) Molecular mechanism of AMPA receptor noncompetitive antagonism, *Neuron 48*, 279−288.
26. Armstrong, N., and Gouaux, E. (2000) Mechanisms for activation and antagonism of an AMPA-sensitive glutamate receptor: Crystal structures of the GluR2 ligand binding core, *Neuron 28*, 165−181.
27. Duggleby, R. G., Attwood, P. V., Wallace, J. C., and Keech, D. B. (1982) Avidin is a slow-binding inhibitor of pyruvate carboxylase, *Biochemistry 21*, 3364−3370.
28. Kulmacz, R. J., and Lands, W. E. (1985) Stoichiometry and kinetics of the interaction of prostaglandin H synthase with anti-inflammatory agents, *J. Biol. Chem. 260*, 12572−12578.
29. Niu, L., Abood, L. G., and Hess, G. P. (1995) Cocaine: Mechanism of inhibition of a muscle acetylcholine receptor studied by a laser-pulse photolysis technique, *Proc. Natl. Acad. Sci. U.S.A. 92*, 12008−12012.
30. Grewer, C., and Hess, G. P. (1999) On the mechanism of inhibition of the nicotinic acetylcholine receptor by the anticonvulsant MK-801 investigated by laser-pulse photolysis in the microsecond-to-millisecond time region, *Biochemistry 38*, 7837−7846.
31. Karpen, J. W., and Hess, G. P. (1986) Cocaine, phencyclidine, and procaine inhibition of the acetylcholine receptor: Characterization of the binding site by stopped-flow measurements of receptor-controlled ion flux in membrane vesicles, *Biochemistry 25*, 1777−1785.

BI700782X

Abstract for the 13th Annual Meeting of the RNA Society
2008, Berlin, Germany

One Aptamer Sequence, Two Structures: A Collaborating Pair that Competitively Inhibits AMPA Glutamate Receptors

Zhen Huang, Weimin Pei, and Li Niu
Department of Chemistry, and Center for Neuroscience Research, University at Albany, Albany, New York 12222, USA

The α-amino-3-hydroxy-5-methyl-4-isoxazole propionic acid (AMPA) subtype of glutamate ion channel receptors plays an essential role in the mammalian brain activities such as memory and learning, whereas excessive receptor activity has been implicated in neurological diseases such as cerebral ischaemia, epilepsy, and amyotrophic lateral sclerosis. Inhibitors acting on AMPA glutamate receptors are drug candidates for potential treatment of these neurological diseases. Using systematic evolution of ligands by exponential enrichment (SELEX), we have identified an RNA aptamer, named as AN58, which competitively inhibits the AMPA receptor with nanomolar affinity. Surprisingly, the *in vitro* transcription of the DNA sequence of AN58 produces two stable RNA structures, M1 and M2, both of which are required for competitive inhibition in a 1:1 stoichiometry. The intrinsic inhibition constant of M1 and M2 was found to be 63 ± 10 nM and 66 ± 18 nM respectively. M1 and M2 are formed independently during the same *in vitro* transcription, but are thermodynamically inconvertible even after they are subject to various denaturing conditions, such as boiling in ~50% formamide containing 7 M urea, and refolding. Using reverse transcription, we show M1 and M2 can be reversely transcribed into the full-length 58-nt cDNA. Sequencing of M1 and M2 using primer extension dideoxy chain termination reaction suggests that they have indeed the same sequence. However, experiments, such as the reverse transcription reaction, which generates different patterns of RT stops, suggest that M1 and M2 have different structures. These findings indicate that the same DNA sequence can be transcribed into two RNA molecules that have the same sequence, but are structurally and functionally distinct. Our results suggest more broadly that natural RNA molecules can evolve to acquire alternative structures and associated functions. Such divergence of RNA phenotype may precede gene duplication at the genome level.